

Unitized Regenerative Fuel Cells (URFCs)

URFC Opportunities and Limitations in the Fields of Space Propulsion and Energy Storage

Completed By:

2Lt. Richard R. Coalson Jr.
17 April, 1998

DISTRIBUTION STATEMENT A

Approved for public release;
Distribution Unlimited

Master of Engineering Space Operations
University of Colorado at Colorado Springs

"All rights reserved. No part of this report may be
reproduced, in any form or by any means, without
permission in writing from the author."

19981119 025

REPORT DOCUMENTATION PAGE

Form Approved
OMB No. 0704-0188

Public reporting burden for this collection of information is estimated to average 1 hour per response, including the time for reviewing instructions, searching existing data sources, gathering and maintaining the data needed, and completing and reviewing the collection of information. Send comments regarding this burden estimate or any other aspect of this collection of information, including suggestions for reducing this burden, to Washington Headquarters Services, Directorate for Information Operations and Reports, 1215 Jefferson Davis Highway, Suite 1204, Arlington, VA 22202-4302, and to the Office of Management and Budget, Paperwork Reduction Project (0704-0188), Washington, DC 20503.

| | | | | |
|---|--|---|--|--|
| 1. AGENCY USE ONLY (Leave blank) | | | 2. REPORT DATE 26.Oct.98 | 3. REPORT TYPE AND DATES COVERED MAJOR REPORT |
| 4. TITLE AND SUBTITLE UNITIZED REGENERATIVE FUEL CESS (URFC) OPPORTUNITIES AND LIMITATIONS IN THE FIELDS OF SPACE PROPULSION AND ENERGY STORAGE | | | 5. FUNDING NUMBERS | |
| 6. AUTHOR(S) 2D LT COALSON RICHARD R | | | | |
| 7. PERFORMING ORGANIZATION NAME(S) AND ADDRESS(ES) UNIVERSITY OF COLORADO AT COLORADO SPRINGS | | | 8. PERFORMING ORGANIZATION REPORT NUMBER | |
| 9. SPONSORING/MONITORING AGENCY NAME(S) AND ADDRESS(ES) THE DEPARTMENT OF THE AIR FORCE AFIT/CIA, BLDG 125 2950 P STREET WPAFB OH 45433 | | | 10. SPONSORING/MONITORING AGENCY REPORT NUMBER 98-034 | |
| 11. SUPPLEMENTARY NOTES | | | | |
| 12a. DISTRIBUTION AVAILABILITY STATEMENT Unlimited distribution In Accordance With AFI 35-205/AFIT Sup 1 | | | 12b. DISTRIBUTION CODE | |
| 13. ABSTRACT (Maximum 200 words) | | | | |
| 19981119 025 | | | | |
| 14. SUBJECT TERMS | | | 15. NUMBER OF PAGES | |
| | | | 16. PRICE CODE | |
| 17. SECURITY CLASSIFICATION OF REPORT | 18. SECURITY CLASSIFICATION OF THIS PAGE | 19. SECURITY CLASSIFICATION OF ABSTRACT | 20. LIMITATION OF ABSTRACT | |

Abstract

Unitized Regenerative Fuel Cells (URFCs) offer a significant advancement in future space system technology. The ability of the URFC to act reversibly as a fuel cell and an electrolyzer allows the integration of two important spacecraft subsystems: power and propulsion. The goal of this paper is to demonstrate the advantages of the URFC system over the separate propulsion and power technology. These advantages will be demonstrated through the compilation of previously documented investigations as well as calculations and scenarios that I have created myself. Overall, I will demonstrate that the efficiency of the integrated URFC system makes it a noteworthy option in spacecraft design.

Table of Contents

| | |
|---|-----------|
| 1.0 Background..... | 4 |
| 2.0 Introduction..... | 6 |
| 2.1 Proton Exchange Membrane (PEM) URFCs..... | 7 |
| 2.2 The URFC Cell..... | 10 |
| 3.0 Specific Topics of Review..... | 14 |
| 3.1 How URFCs Compare to Batteries..... | 15 |
| 3.2 The H ₂ /O ₂ Propulsion System..... | 20 |
| 3.3 Safety of the URFC System..... | 24 |
| 3.4 Mission Example..... | 26 |
| 4.0 Discussion of Limitations..... | 43 |
| 5.0 Discussion of Applications..... | 44 |
| 5.1 IMPRESS System for Small Satellites..... | 45 |
| 6.0 Conclusion..... | 47 |
| Appendix A..... | 48 |

1.0 Background

Fuel cells generate electricity through an electrochemical process in which the energy stored in a fuel is converted directly into DC electricity, without combustion. All fuel cells operate with the same basic principles. An input fuel is catalytically reacted in the fuel cell membrane to create an electrical current. This current is induced by the cells which are composed of an electrolyte material which is sandwiched between two thin electrodes. If the fuel cell is designed to operate in reverse as an electrolyzer, then this dual-function system is known as a reversible fuel cell (RFC) or a unitized regenerative fuel cell (URFC). URFCs were developed because of the mass savings which could be accomplished over a separate electrolyzer and fuel cell system [1].

There are four primary types of fuel cells which are named for the type of electrolyte employed. These fuel cell types and their more important characteristics are listed in Table 1.

| | Phosphoric Acid (PA) | Molten Carbonate (MC) | Solid Oxide (SO) | Proton Exchange Membrane (PEM) |
|-----------------------|--------------------------------------|--------------------------------------|--|---------------------------------------|
| Electrolyte | Phosphoric Acid | Molten Carbonate Salt | Ceramic | Polymer |
| Operating Temperature | 375° F (190° C) | 1200° F (650° C) | 1830° F (1000 °C) | 175 °F (80° C) |
| Fuels | Hydrogen (H ₂) Reformate | H ₂ /CO Reformate | H ₂ /CO ₂ /CH ₄ Reformate | Hydrogen (H ₂) Reformate |
| Oxidant | O ₂ /Air | CO ₂ /O ₂ /Air | O ₂ /Air | O ₂ /Air |

Table 1. Characteristics of some of the most common fuel cell technologies [1].

Proton exchange membrane (PEM) fuel cells offer the most promising technology for space-based applications because of their low operating temperature, their efficient energy storage capacity, and their use of H₂ and O₂ as a fuel source. PEM hydrogen-oxygen fuel cell technology will be the emphasis of this paper. At times, the paper will refer to the PEM as a solid polymer electrolyte (SPE) fuel cell. Both names refer to the same technology; however, (SPE) has been registered as a trademark of the Hamilton Standard division of United Technologies Corporation [2].

Fuel cells have been flight proven in space programs since the 1960s when they supplied on-board power for the Gemini and Apollo spacecraft [3]. Today, their use is prevalent in power plants, zero emission vehicles, and they are used as a source of on-board power for the Space Shuttle. However, very few of these applications use the currently developed unitized regenerative fuel cells (URFCs). To date, URFCs are not space qualified because the usefulness of their reversible technology was not discovered early in fuel cell development. Added to this, funding for research has been limited. However, PEM technology is developing rapidly and is expected to gain official acceptance into the field of space within the next couple of years [4].

2.0 Introduction

The URFC system achieves its efficiency by combining the tasks of both the propulsion and power (battery) subsystems. As a fuel cell, the URFC provides DC power to the spacecraft from stored gaseous hydrogen and oxygen. As an electrolyzer, the URFC uses electrical power to produce hydrogen and oxygen from stored water. The gaseous hydrogen and oxygen provide high specific impulse (I_{sp}) rocket bipropellants and cold gas attitude control propellants. The URFC integrated propulsion system, storing its propellants solely as water, has earned the nickname the "water rocket". These propellants are created as required by the mission, allowing for an on-the-fly trade between the propulsive capacity and the stored energy capacity.

The URFC offers substantial advantages over the separate battery and propulsion system. A few of the major areas include: 1) reduced spacecraft wet and dry mass, 2) increased mission safety with storable, high performance non-toxic propellants, 3) increased mission flexibility via trades in delta-velocity (ΔV) maneuvering versus stored energy capacity, and 4) utilization of unspent propellants for additional energy storage [2].

The above advantages will be explored throughout this paper. First, a comparison will be made between the URFC technology and batteries in the field of energy storage. Second, an evaluation of the gaseous H_2/O_2 propulsion system will be performed. Third, the safety of the entire URFC propulsion/power system will be explained. Finally, to tie it all together, I have created a hypothetical mission and demonstrated URFC technology with it.

Together, these separate investigations will fully demonstrate the URFC's efficiency in space applications. Before comparisons can begin, it is necessary to have a firm understanding of the URFC system.

2.1 Proton Exchange Membrane (PEM) URFCs

The URFC technology that is described within this report is the hydrogen-oxygen fueled proton exchange membrane (PEM) or solid polymer electrolyte (SPE) fuel cell. This fuel cell has the dual capability of producing gaseous oxygen and hydrogen for use as a bipropellant and recombining them to produce electrical power. The URFC does this efficiently through a proton exchange membrane composed of a single stack of reversible cells. The sulfonic acid membrane electrolyte is formed into cells by bonding catalyst electrodes to both faces of the membrane [2]. The membrane itself is made of polyperfluorosulfonic acid and is somewhat similar to DuPont's Teflon, more specifically their product labeled Nafion 120 [5]. The catalyst is formed by mixing platinum and platinum-group metals with their oxides [6]. The resulting bifunctional oxidation and reduction electrodes have the capability to reverse roles when switched from charge to discharge, similar to a rechargeable battery [3]. The reversible aspect of the cells make them highly efficient. Their versatility not only eliminates the excess weight of two separate membranes, but it also eliminates the additional components and plumbing that would be required in a separate electrolyzer and

generator system. A diagram of the electrochemical reactions that occur in the SPE URFC are shown below in Figure 1.

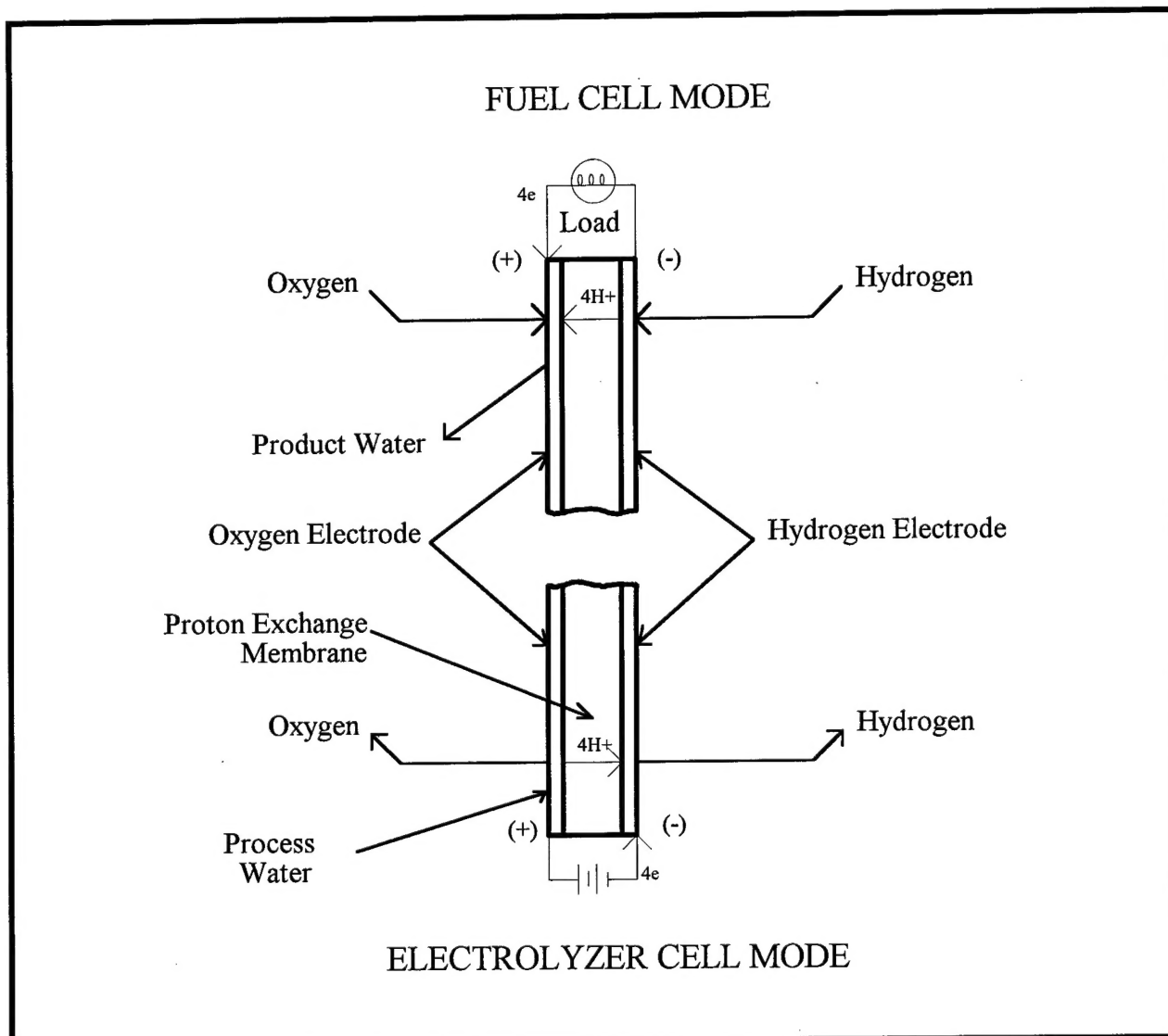


Figure 1. A simplified schematic of the SPE unitized regenerative fuel cell (URFC) [2].

As shown above, the two separate URFC modes of operation are termed the electrolyzer mode and the fuel cell mode. The electrolyzer mode uses an external power supply to split water

into gaseous oxygen and gaseous hydrogen. An electrical current is channeled through a solution of sulfonic acid and water, and the added energy causes the water to break up and form H₂ and O₂. Specifically, the electrical current oxidizes the water at the anode by withdrawing electrons, and the current reduces the water at the cathode by adding electrons. The following oxidation and reduction half-reactions are shown in Figure 2. Notice that recombination also occurs, but this does not have any negative effect on the reaction:

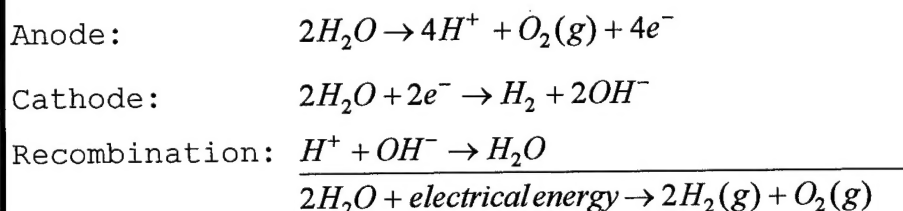


Figure 2. The Electrolyzer Mode.

In the fuel cell mode of operation, electrical energy is produced through the chemical combination of gaseous H₂ and O₂. As shown in Figure 3, the H₂ gives up electrons as it is oxidized and the O₂ takes up electrons as it is reduced. A byproduct of this reaction is heat, and this should be accounted for in spacecraft design.

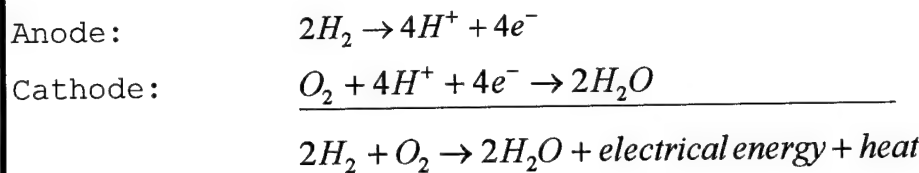


Figure 3. The Fuel Cell Mode.

2.2 The URFC Cell

The PEM/SPE URFC system must not only produce gaseous H₂ and O₂ from water, but it must keep all of the components separated during the process. The URFC cell is the building block of the URFC system. The cell's structure is divided into four chambers: oxygen, hydrogen, product water, and process water. The series of membranes within the cell allow the process and product water to be transported passively back and forth from the cell to the storage tanks. Figure 4 shows a simplified schematic of a SPE URFC fuel cell.

Added to the structure, the reversible cell must have a reliable transfer mechanism for both the gasses and liquids in both directions, allowing for its use both as an electrolyzer and a fuel cell. On the ground, this feat can be accomplished with relative ease, but there are additional challenges in a microgravity environment. Remember, it is also important to keep the mass down on any spacecraft, and all of the parts must be reliable and maintenance-free for the duration of the mission.

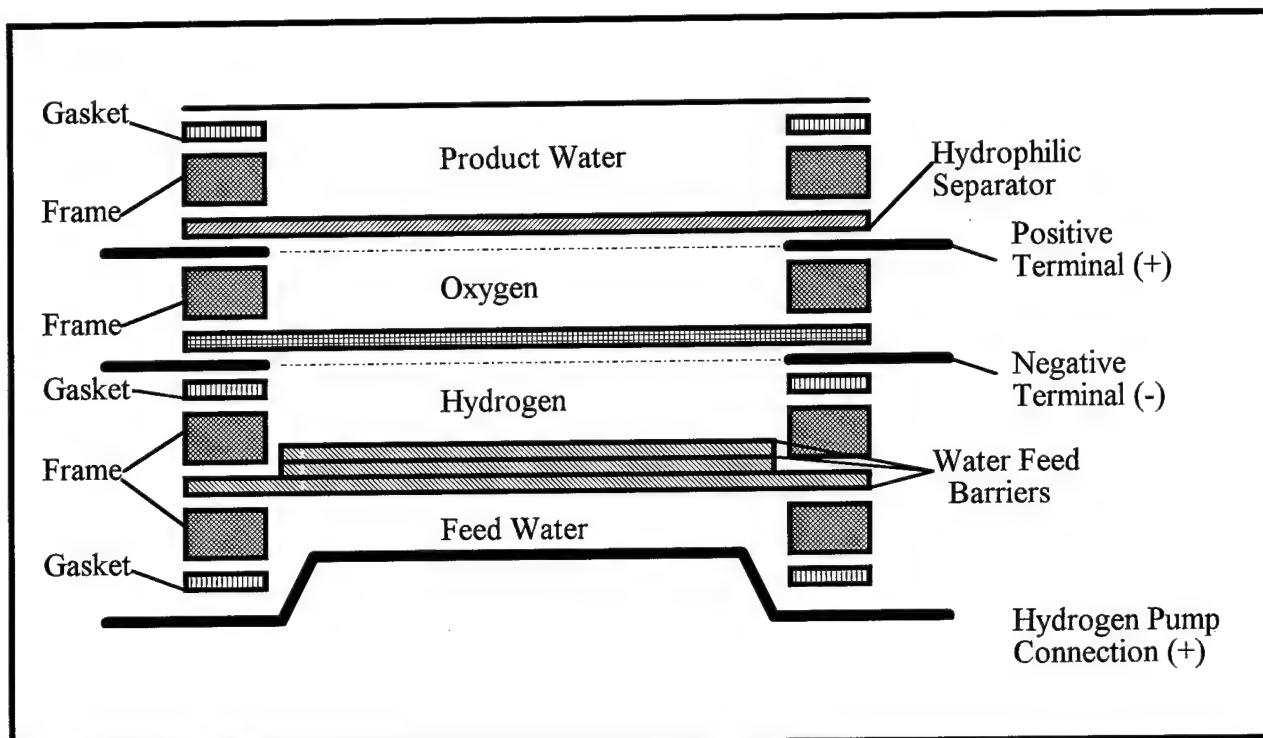


Figure 4. Individual Cell Structure for a SPE URFC [2].

The SPE URFC accomplishes the above challenges through passive phase separations, relying only on electrochemically generated differential pressures to distribute the reactant and product fluids to and from the storage tanks [2]. Specifically, water vapor is supplied to the cell during the charge electrolysis period passively, liquid product water is removed from the cell during the fuel cell discharge period passively, and gas is eliminated from the water side of the water vapor barrier membrane passively. This enhances the system because there are no pumps or rotating equipment that may wear out or malfunction during the mission.

The SPE URFC simplified fluid schematic shown in Figure 5 illustrates the transfer of water, O₂, and H₂ throughout the system. In the fuel cell mode of operation, unregulated gaseous O₂, and H₂ are delivered to the cell as demanded by consumption. Product water is released on the oxygen side of the cell, contacts the hydrophilic porous membrane, and is transferred to the water/oxygen tank for storage by a forced differential pressure. This forced differential pressure is provided by the spring bellows, and is typically one pound per square inch. To ensure that the product water is free of gaseous or dissolved oxygen and hydrogen, it is passed through the water side of the electrochemical hydrogen pump. Also shown in Figure 5, thermal interfaces border the cell to carry waste heat away from the cell [2].

Again referring to Figure 5, the electrolysis mode of operation is similar to the fuel cell mode of operation. In the electrolysis mode, feed water (free of dissolved gasses) enters the water side of the electrochemical hydrogen pump cell membrane and is transported to the operating electrolysis cell by osmosis. Osmotic transport is aided by proton pumping, as four water molecules are pulled across the membrane with each passing proton. When the water vapor reaches the electrolyzer cell, it returns to its liquid state before it is reacted to produce gaseous hydrogen and oxygen.

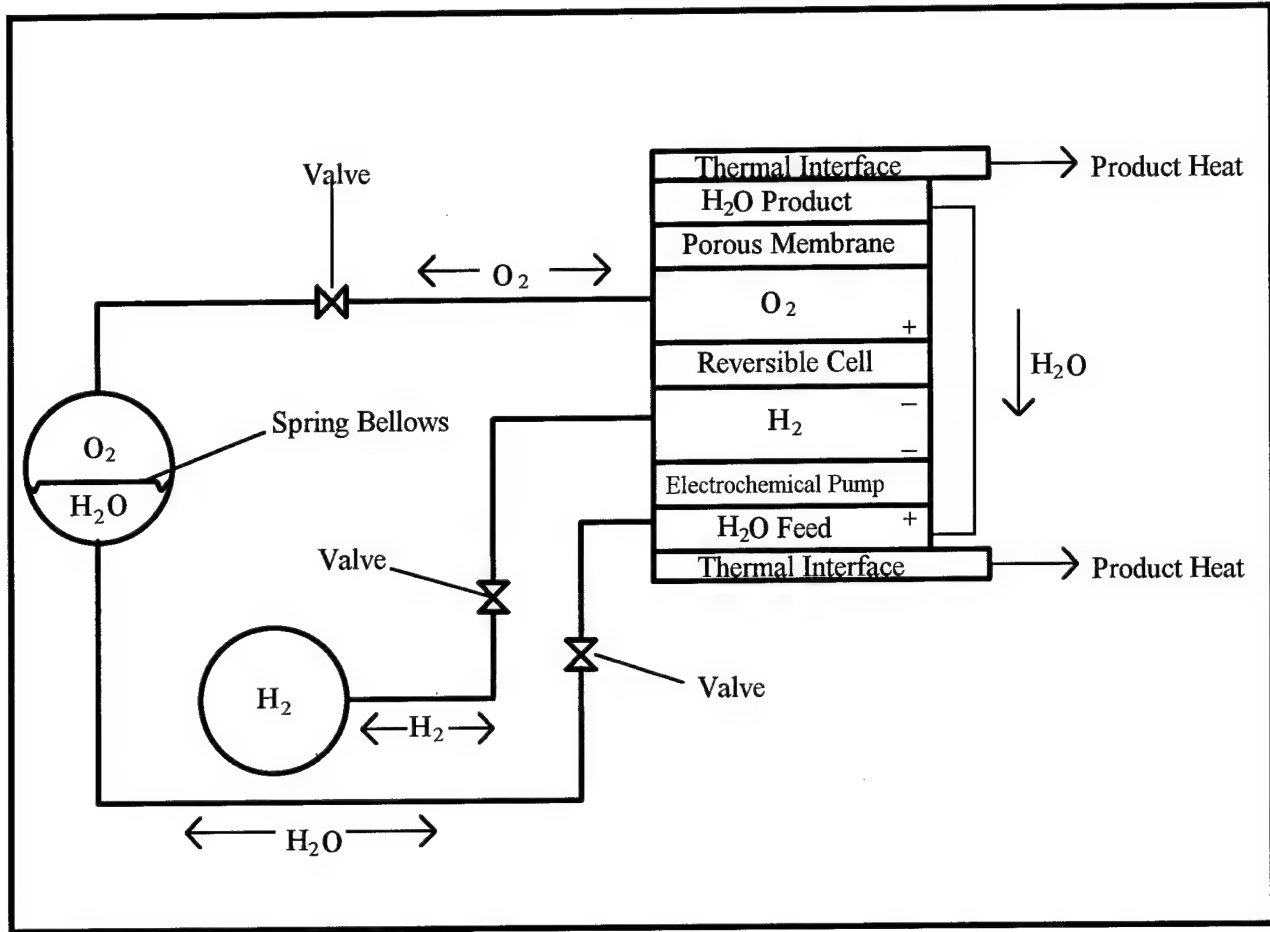


Figure 5. SPE URFC System Fluid Schematic [2].

Referencing Figure 6, it is important to note that the water is in the gaseous form as it crosses through the oxygen chamber. This is also true when the water passes through the hydrogen chamber, and this allows instantaneous switching of fuel cell and electrolyzer modes of operation. Also, this eliminates the possibility of the water freezing in the H_2 and O_2 storage tanks and transport lines.

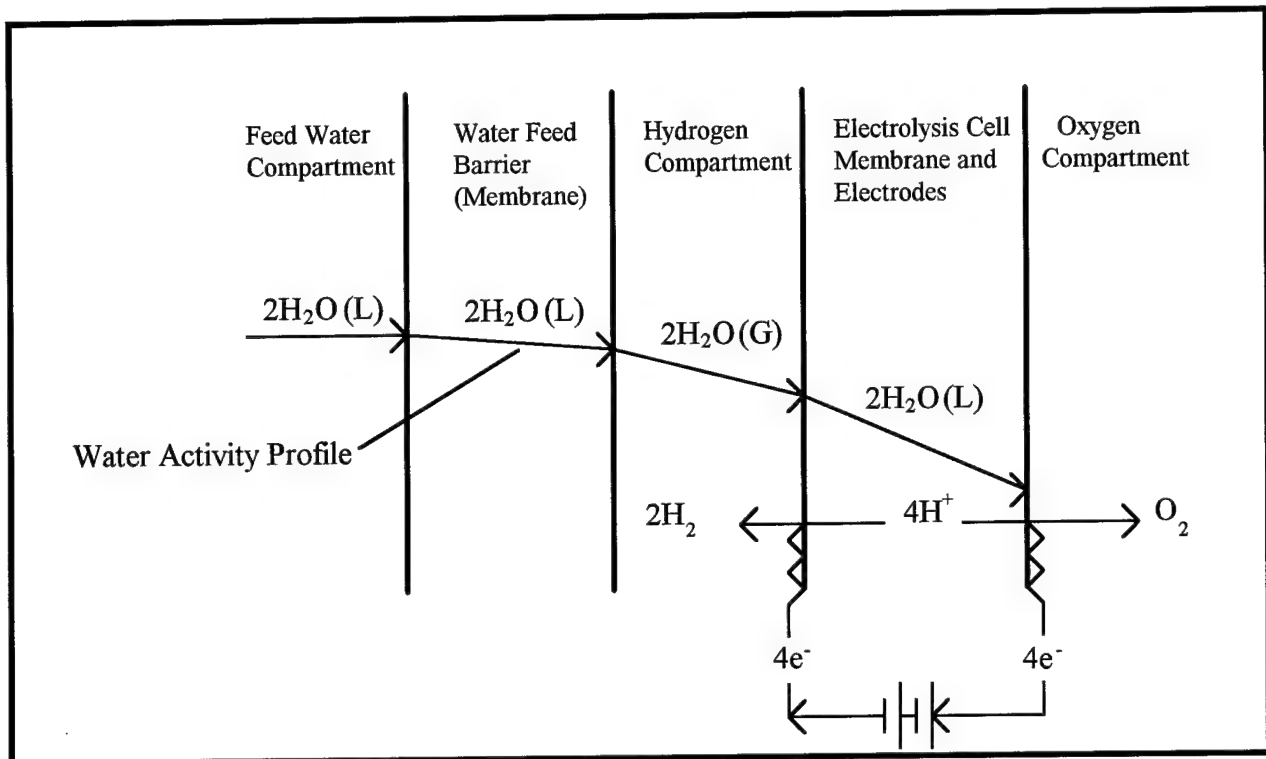


Figure 6. Fundamentals of Water Vapor Feed Electrolysis [2].

3.0 Specific Topics of Review

The only way to demonstrate a system's ability is to directly compare it to its competition, noting advantages and disadvantages between the competing technologies. This approach will be applied through the documentation of prior research and the introduction of new information which has been created specifically for this paper. All of the calculations which have been performed within this report are considered to be accurate only for an initial system design. Relatively, the numbers provide a great deal of information about the competing technologies; however, the exact design parameters would require a more detailed assessment of the system. The specific topics which will be discussed are: the comparison between URFCs and

batteries, the gaseous H₂O₂ propulsion system, the safety of the URFC system, and a mission example which applies URFC technology.

3.1 How URFCs Compare To Batteries

Battery and other energy storage systems are often rated by how efficiently they can store energy with respect to their system mass. Table 2 allows us to compare the specific energy values of a variety of state of the art batteries to that of a URFC. The specific energy values are given in units of watt-hour per kilogram (Wh/kg), and this represents the capacity of the battery per unit weight.

For this comparison, it is important to understand exactly what is being represented. First, the values do not include the weight of the solar arrays needed to charge the batteries or URFCs, and these omitted values are assumed to be similar for all of the electrical storage systems. Secondly, the URFCs listed in the table are stand-alone, implying that they have not been integrated into the propulsion system yet. Finally, it is important to differentiate between the theoretical and packaged specific energy. The theoretical specific energy is based solely on the chemical reactions that occur within the electrical storage system. These values only include the weight of the materials that compose the individual cells of the battery, and they neglect the packaging materials needed to contain and manage the active portion of the system. Although these theoretical values do not aid in design, they do allow us to see which technologies are difficult to package.

| Battery/URFC System | Theoretical Specific Energy (Wh/kg) | Packaged Specific Energy (Wh/kg) | Comments |
|-------------------------------------|-------------------------------------|----------------------------------|---|
| H ₂ /O ₂ URFC | 3660 | 400-1000 | URFCs with light-weight pressure vessels |
| Li-SPE/MO _X | 735 | 220 | Novel packaging for unmanned systems |
| Ag/Zn | 450 | 200 | Excess Zn required, low charge rate |
| Li/LiCoO ₂ | 735 | 150 | Poor cycle life, high capacity fade |
| Li/AlFeSe ₂ | 515 | 150 | ≥400°C thermal management |
| Na/S | 1180 | 150 | ≈350°C thermal management |
| Li/TiS ₂ | 470 | 130 | ≈50% DOD for high cycle life (900 cycles) |
| Li/ion | 700 | 100 | Marginal improvement for larger cells |
| Ni/Zn | 305 | 90 | Excess Zn required, low specific energy |
| Ni/MH _X | 470 | 70 | MH _X is metal hydride Low specific energy |
| Ni/H ₂ | 470 | 60 | Low specific energy |
| Ni/Cd | 240 | 60 | Low specific energy |
| Pb/acid | 170 | 50 | Low specific energy |

Table 2. Theoretical and Packaged Specific Energy for URFCs and State of the Art Rechargeable Batteries [2].

In addition to the specific energy advantage of the URFC over state of the art battery systems, the URFC's capacity does not vary with the depth-of-discharge (DOD). The depth-of-discharge measures the percent of the total battery capacity removed during a discharge period. Higher percentages allow less total required battery capacity; however, higher percentages also limit the lives of the batteries. To explain this problem, it is important to look at how the capacity of a battery system is calculated. Notice that DOD is in the denominator of the equation, and as the value of DOD increase towards 100 percent, the required mission battery capacity is reduced. Figure 7 shows an equation used in *Space Mission Analysis and Design* to determine the capacity of a battery system in watt-hours.

$$Cr = \frac{P_e T_e}{(DOD) N n} (W-hr)$$

Parameter Descriptions

Cr = Required battery capacity in W-hrs per battery

P_e = Average eclipse load (W)

T_e = Maximum eclipse time (hr)

DOD = Limit on battery's depth-of-discharge

N = Number of batteries (non-redundant)

n = Transmission efficiency between battery and load

Figure 7. Estimate of the Required Capacity of Secondary Batteries [8].

Figure 8, adapted from *Space Mission Analysis and Design*, illustrates the relationship between the average depth-of-discharge and the cycle life. Notice that there is an exponential loss in the allowable discharge capacity as the life of the battery is increased. This translates into the need for a larger battery, using less of its capacity for the mission. Overall, this wastes valuable mass on the spacecraft.

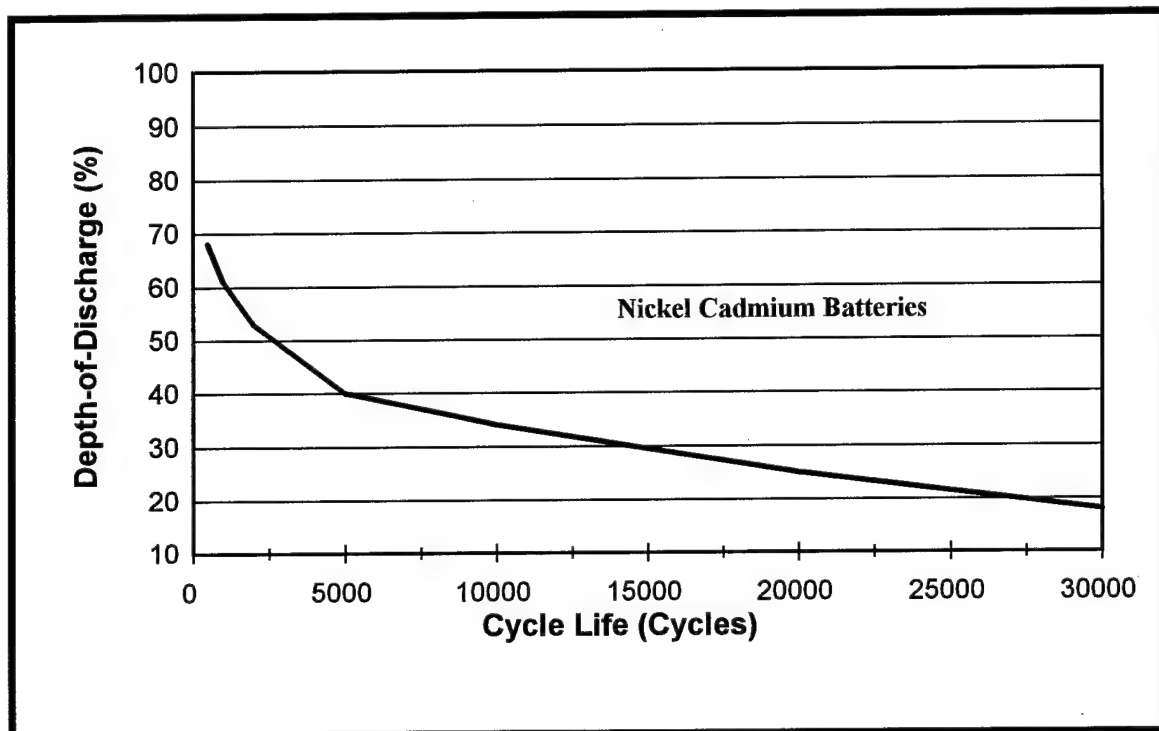


Figure 8. Depth-of-Discharge Versus Cycle Life for Nickel Cadmium Batteries [7].

In contrast to battery systems, the URFC is unaffected by the depth-of-discharge or cycle length. In the URFC, energy and power are uncoupled. The reactor stack is sized only for power,

and the H₂ and O₂ storage tanks are sized for energy. Specifically, a 20 kW reactor stack will be the same size regardless of whether the discharge time is one minute or one year. Figure 9 shows the mass penalties associated with the depth-of-discharge percentage of nickel cadmium (NiCd) batteries. For this comparison, all of the parameters on the right-hand side of the equation in Figure 7 were held constant except for DOD. The resulting mission battery capacities were multiplied by the energy density of NiCd batteries listed in Table 2 (60 W-hr/kg) to arrive at a battery mass.

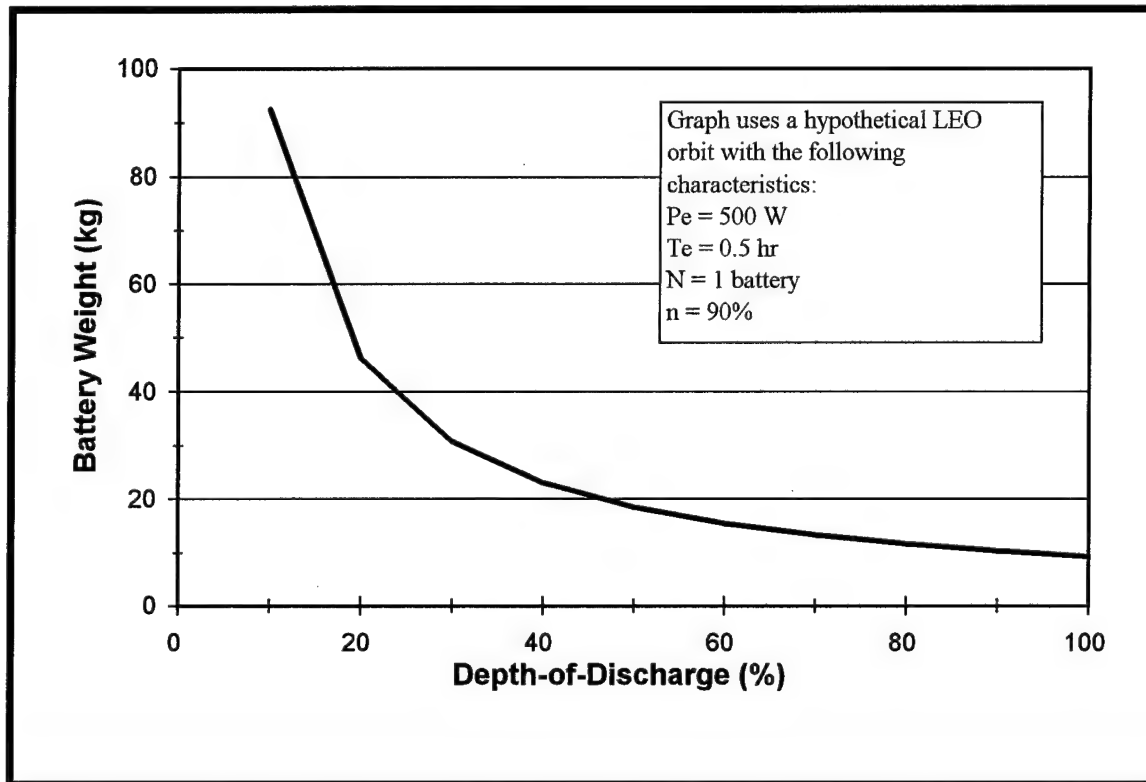


Figure 9. Battery mass versus the allowable depth-of-discharge.

Finally, the URFC systems require less regulation than battery systems. The only areas which need to be regulated are the water tank temperature so that the water does not freeze, the pressure in the storage tanks, and alternation between the fuel cell or electrolyzer modes of operation. The temperature problem is virtually solved because the URFC system has an operating temperature of 80°F, and the heat can be radiated around the storage tanks. Unlike batteries, URFCs do not have to avoid the problems with overcharging, charging imbalances, or having the system develop a memory. Overcharging batteries quickly degrades their performance, and not fully discharging the batteries can cause them to develop a memory. A "memory", is a degradation of a battery's performance which reduces its capacity to that which is frequently demanded.

3.2 The Gaseous H₂/O₂ Propulsion Subsystem

One of the greatest advantages of the hydrogen/oxygen fuel cell is that it provides a very high quality propellant for the propulsion subsystem. The most common performance parameter used for propulsion is the specific impulse (Isp). The specific impulse compares the thrust achieved from a system as a function of the propellant mass flow rate, as shown in Figure 10:

$$I_{sp} = \frac{F}{\dot{m}g_0}$$

where I_{sp} = specific impulse (s)
 F = thrust magnitude (N)
 \dot{m} = propellant mass flow rate (kg/s)
 $g_0 = 9.807 \text{ (m/s}^2\text{)}$

Figure 10. The specific impulse equation and its parameters [8].

From this equation, a standardized value of seconds can be used to evaluate any propellant, no matter what fuel or oxidizer is used. The higher the I_{sp} , the more fuel efficient the propellant is. Taking this knowledge and the results from *Space Propulsion Analysis and Design*, it is possible to see how gaseous hydrogen and gaseous oxygen used as a bipropellant stack up to other common chemical technology propellants. First, it is important to explain that the gaseous hydrogen/oxygen mixture burns exactly the same as their liquid counterparts. Chemically, the same products and reactants are involved, and the same results are expected; however, for a direct comparison, the ratio of the oxidizer to the fuel must be the same in both cases.

Figure 11 illustrates the effect that the oxidizer to fuel mass ratio (O/F) has on the I_{sp} . The area labeled "typical value" relates to the O/F ratio commonly used on liquid-type launch vehicles. From the curve, it is easy to see that they are trying to maximize the I_{sp} . The line labeled "water rocket" designates the O/F ratio where all of the propellants produced by the fuel cell will be used. This I_{sp} shift can be related to a turbocharger on an automobile; the more air you compress into the

engine (oxidizer), the more complete combustion and power you get out of it (I_{sp}). Notice that there is a point where adding oxidizer starts to reduce the performance.

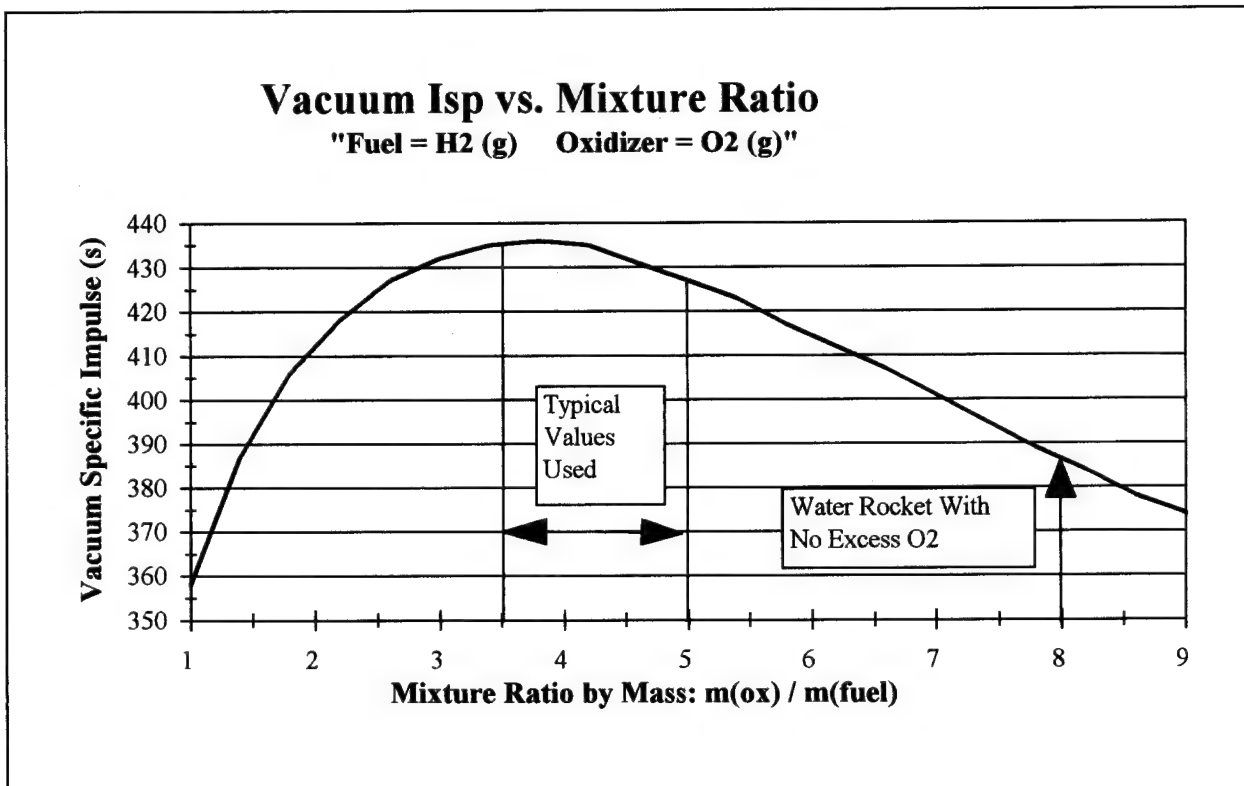


Figure 11. The effects of the O/F mixture ratio on the specific Impulse of H₂/O₂ bipropellant propulsion system. The water rocket can be designed to produce any of the O/F ratios above [8].

The water rocket propulsion system allows the engineer to decide what I_{sp} they want to design for, remembering that they can control the (O/F) ratio. As mentioned above, the URFC produces fuel at an O/F ratio of 8:1 because each H₂O molecule produces two hydrogen molecules together at 2kg/kg-kgmol and one oxygen molecule at 16 kg/kg-mol. Looking again at Figure 11, an

O/F ratio of 8:1 sacrifices much of the possible I_{sp} ; however, the engineer does not have to design a system to store or outgass the excess oxygen. Typically, a satellite engineer does not want anything outgassing from the satellite, so the 8:1 O/F ratio might offer the best solution. On a manned mission scenario, the excess oxygen could easily be used for life support functions, increasing the I_{sp} at the same time. Lastly, if the engineer wants to use some of the URFC's H₂ as the propellant in a cold gas thruster for attitude control and orbit maintenance, they must decide what to do with the excess oxygen.

Table 3 gives a comparison of I_{sp} values for some of the more common chemical propellants used today in rocket technology.

| Chemical Technology | Specific Impulse (I_{sp}) in Seconds |
|---|--|
| Liquid Fluorine/Hydrogen | 390-440 |
| Gaseous or Liquid Hydrogen/Oxygen | 360-435 |
| Gaseous Hydrogen/Oxygen Burnt at an O/F of 8:1 | 385 |
| All Other Liquid Bipropellants | 320-360 |
| All Hybrid Technologies | 290-350 |
| All Solid Technologies | 260-300 |
| All Liquid Monopropellants | 140-235 |

Table 3. A comparison of I_{sp} values for chemical propellants [8].

Notice that the only category of chemical rocket technology that beats the gaseous (H_2/O_2) combination is the liquid fluorine/liquid hydrogen (F_2/H_2) bipropellant. Because of fluorine's extreme toxicity and the environmental damage that it causes the atmosphere, its use is currently banned. Overall, the propellants produced in the URFC-based water rocket provide very efficient and high performance fuel.

3.3 Safety of the URFC System

The water rocket's concept of using gaseous hydrogen and oxygen as the spacecraft's propellants has virtually eliminated many of the common problems with current propulsion technology. Some of the current propellant downfalls include problems with stability, handling, storage, and compatibility with container materials. For example, liquid oxygen and liquid hydrogen are cryogenic, and hydrazine, nitrogen tetroxide, and fluorine are very toxic. Gaseous hydrogen and oxygen are not toxic, and pose very few problems with stability or container compatibility. The problems with storage and handling are alleviated because the water rocket stores its propellants as water until after launch. There is no current system with this level of safety on the market today.

Given today's environmental laws, safety requirements, and liability fears, it is extremely difficult or impossible to develop new rocket technology if toxic propellants are involved. Conventional spacecraft propulsion technology is mature and proven, and it is forced to avoid much of the risk of new

development. The number of facilities in the U.S. where toxic rocket propellant testing is allowed is decreasing due to the increased costs that come with new environmental regulations and higher safety standards. The tests that are performed have been limited to those of proven systems which have only slight modifications. Although these tests are very likely to succeed, they only allow very limited and slow growth in the overall rocket technology. Each test is very extensive because very few tests are allowed. As each test becomes more important, the levels of accuracy, redundancy, and expense increase. Overall, this approach is not conducive to radical propellant system advances [2].

In comparison, non-toxic testing strategies have the ability to embrace revolutionary technology. It is the basic risk versus return model, and as testing with non-toxic propellants allows larger risks, the returns in technological advancement are greater. Frequent, low-cost, high-risk tests can be accomplished without the financial and liability burdens which accompany toxic testing. With this, data and testing are no longer the limiting factors, but they become the driving factors in technological development [2].

Another downfall with toxic propulsion systems is that field testing and integrated system testing have been limited greatly due to environmental and safety guidelines. In an effort to avoid the cost and complexity of these complete system tests, designers are forced to overemphasize the importance of the flight heritage of the individual spacecraft components. With

this current trend, new technology is put on hold until it can find a way to gain flight heritage. Although flight heritage is very important in non-toxic systems such as the water rocket, it is much easier to promote system testing if the safety of the propellant system is high [2].

Finally, the water rocket stands alone in safety during the launch segment of the mission. Stored as water, the propellant poses no threat to the launch site or its personnel. The factors of safety on the tanks, welding, and plumbing can be greatly reduced saving time, money, and spacecraft dry mass. These factors of safety are especially important when the propellant is handled at the launch site and on manned missions. For example, any spacecraft catching a ride on the Space Shuttle would have to account for higher safety standards, especially if it contained toxic materials [2].

3.4 Mission Example

In order to investigate the advantages of using a hydrogen-oxygen fuel cell in the propulsion system, I created a hypothetical mission that needs to transfer a satellite from a low altitude earth parking orbit (LEO) to a geostationary orbit (GEO). The orbits were selected as circular orbits with matching inclinations so that the maneuver could be accomplished with a simple Hohmann transfer. The spacecraft mass that I chose for the mission was similar to that of the Landsat 4 series of satellites at 3600 kg. This mission is not the most practical mission in theory because most satellites of this size would

achieve a GEO orbit via an upper stage of the launch vehicle; however, I chose a mission which required a large change in velocity (ΔV) in order to emphasize the mass and fuel savings. It is important to note that this example is particularly relevant to any other mission with a similar ΔV requirement, and the results may be scaled down for smaller missions.

The focus of my analysis is the savings in spacecraft wet and dry mass through the use of the URFC-based gaseous hydrogen and oxygen propulsion system. The URFC water rocket technology was compared to that of hydrazine. Hydrazine is one of the most commonly used propellants for post-launch satellite maneuvering. Specifically, the key areas which separate the two competing technologies include: differences in the propellant I_{sp} values, the size and weight of the storage tanks, the ability to eliminate a pressurant system, and the difference in inert masses.

In order to focus on these areas, a few simplifying assumptions were made. First, since the storage tanks are the most significant portion of the propulsion system mass summary, the other hardware components are ruled negligible. This is a reasonable assumption because the two technologies will have similar components, and for the same mission, they will be very close to the same in mass. These components include items such as the nozzle, the thrust chamber, the plumbing, and even the weight of the URFC itself. Secondly, body mounted solar arrays were assumed for the mission. Solar arrays must be used to create fuel for the Hohmann transfer maneuvers; however, they

cannot be extended during the thrust maneuvers. This would not only put an undo amount of stress on the extended solar arrays, but the extended appendages could create an attitude control nightmare during the thrust. This is a practical assumption even if the body mounted solar arrays do not provide the required energy to promptly create the propellants. In this situation, the satellite would have to postpone its maneuver in a phasing orbit until the URFC had recharged it's fuel tanks.

The mission itself starts with the Hohmann transfer, offering the lowest energy transfer between the two orbits.

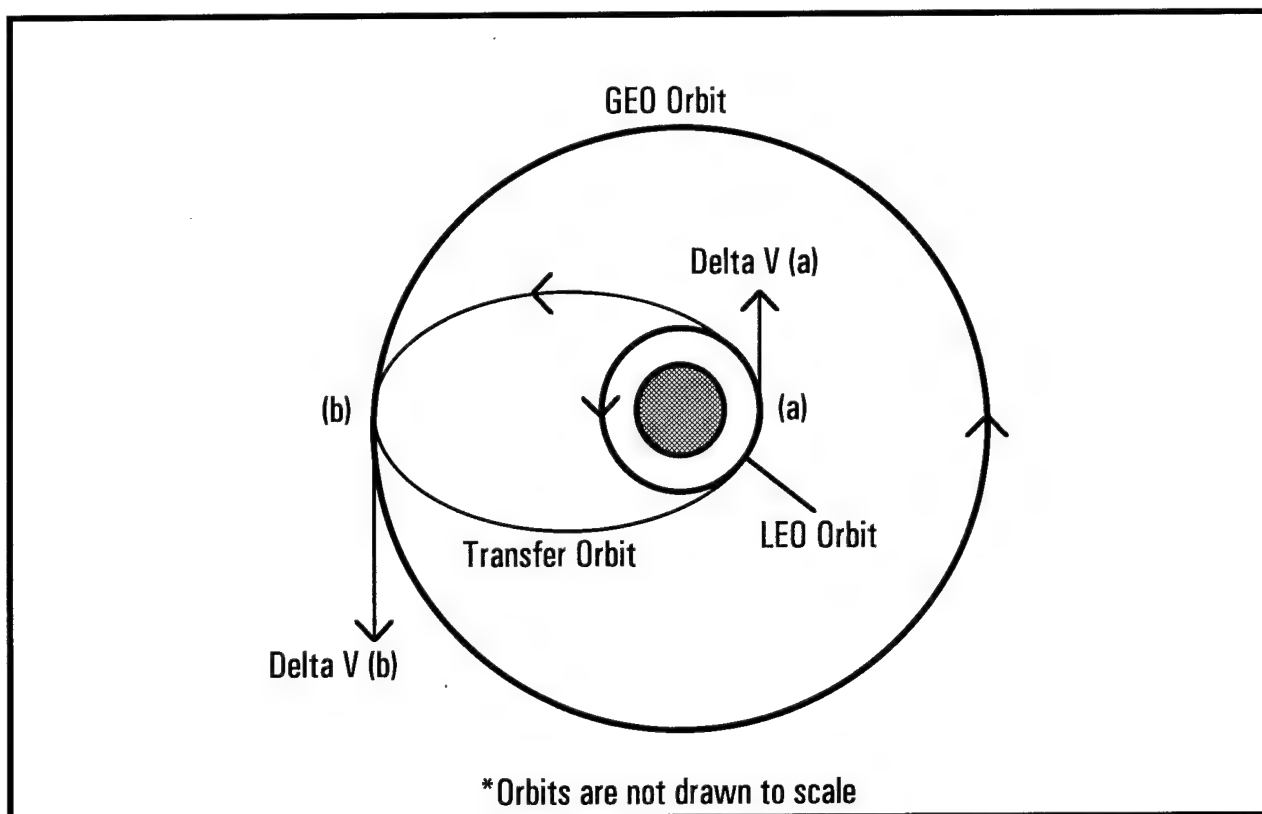


Figure 12. The Hohmann Transfer is a two-impulse minimum change in velocity maneuver. The elliptical transfer must start at either apogee or perigee for this maneuver to be minimum.

In order to use a Hohmann transfer it is necessary to make the following assumptions: 1) the burns occur instantaneously, 2) the burns are coplanar, 3) the burns are tangential to the orbit plane, and 4) the flight path angle is zero at the time of the burn. The mission was designed to meet these criteria. Figure 12 shows the original orbits, the elliptical transfer orbit, and the two separate burns needed to accomplish the mission. The altitude of the LEO orbit was 222 km and the altitude of the GEO orbit was 35,780 km. Table 4 illustrates the algorithm that was used to find the required mission ΔV .

The Hohmann transfer algorithm produces a ΔV that is used to size the rest of the spacecraft propulsion subsystems. The first step in this process is to use the ideal rocket equation to calculate the mass of propellant needed. At this point we have almost all of the design parameters; we have the fuel's Isp, the payload mass, and the delta-V required. The factor that has to be assumed is the inert mass fraction

The inert mass accounts for all of the spacecraft components which are neither propellant nor included within the payload. The inert mass estimate was made from prior missions, and typical values of the inert mass fraction range from 10% to 25%. In general, the lower the percentage, the more efficient the rocket's structure has to be, and the more difficult and expensive the rocket is to design and build. With higher percentages, the design becomes easier and cheaper, but the overall mass of the spacecraft may grow too large.

| Value | Symbol | Equation | Units | Mission Results |
|--------------------------|---------------------------|--|--------------------------|-----------------|
| LEO Radius | R_i | Given | km | 6600 |
| GEO Radius | R_f | Given | km | 42158 |
| Gravitational Parameter | μ | Constant | km^3/s^2 | 398600.4415 |
| Transfer Semi-major axis | a_{trans} | $\frac{R_i + R_f}{2}$ | km | 24379 |
| Initial Velocity | v_i | $\sqrt{\frac{\mu}{R_i}}$ | km/s | 7.771 |
| Final Velocity | v_f | $\sqrt{\frac{\mu}{R_f}}$ | km/s | 3.075 |
| Transfer Velocity (a) | $v_{\text{trans-a}}$ | $\sqrt{\frac{2\mu}{R_i} - \frac{\mu}{a_{\text{trans}}}}$ | km/s | 10.219 |
| Transfer Velocity (b) | $v_{\text{trans-b}}$ | $\sqrt{\frac{2\mu}{R_f} - \frac{\mu}{a_{\text{trans}}}}$ | km/s | 1.600 |
| Delta-V at Point (a) | Δv_a | $v_{\text{trans-a}} - v_i$ | km/s | 2.448 |
| Delta-V at Point (b) | Δv_b | $v_{\text{trans-b}} - v_f$ | km/s | 1.475 |
| Total Delta-V | Δv_{total} | $ \Delta v_a + \Delta v_b $ | km/s | 3.923 |
| Transfer time | τ_{trans} | $\pi \sqrt{\frac{a_{\text{trans}}^3}{\mu}}$ | s | 18,941.08 |

Table 4. Hohmann transfer algorithm and mission calculations [9].

To check to see whether the inert mass fraction is feasible for a particular mission, a Dummkopf chart is created. The Dummkopf chart creates a series of curves which compare the Isp of the rocket fuel to the initial mass of the vehicle. By

looking at the I_{sp} of the propellants chosen, we reference a location on the set of curves. Each of the separate curves represent a separate inert mass fraction. If the propellant's I_{sp} value intersects a curve where it is relatively flat or smooth, then the design is acceptable. As the I_{sp} value is lowered, the curve becomes steeper and design is more risky, or perhaps impossible.

The design risk is best explained by considering a small fluctuation in the actual I_{sp} value from your design value. Where the curve is steep, this small fluctuation causes a huge change in initial mass, and this may result in an impossible mission scenario. Where the curve is flat or smooth, a small fluctuation in the actual I_{sp} value would result in a minimal fluctuation in the initial mass. The Dummkopf Chart technique was introduced by Captain Michael Bettner in the fall semester of ASE 521 (Rocket Propulsion) at the University of Colorado at Colorado Springs.

The spreadsheets and resulting Dummkopf charts for this mission analysis are located in Appendix A. These were created after the design had been completed to check the initial estimate of the inert mass fraction. There are two separate Dummkopf charts, one for each of the hydrazine and H_2/O_2 technologies. I have chosen the design I_{sp} values of 230 seconds for Hydrazine and 385 seconds for H_2/O_2 based on recorded values presented in *Space Propulsion Analysis and Design*. Notice that the hydrazine design value intersects the curve in a much steeper region, forcing a lower inert mass fraction and increasing the risk of

design. The H₂/O₂ system, on the other hand, intersects the curve in a very smooth portion. This allow the designer to incorporate a more practical inert mass fraction and have more confidence in the results. In this mission analysis, an inert mass fraction of 12% was chosen for hydrazine and 18% for H₂O₂.

The algorithm that was used to generate the data points for the Dummkopf charts is listed below. Notice, that this algorithm also gives us the inert, initial, and final spacecraft mass.

| Step Description | Symbol | Corresponding Equation | Units |
|---------------------|--------------------|---|-------|
| ΔV Required | ΔV | Given | (m/s) |
| Inert Mass Fraction | f _{inert} | Chosen | none |
| Payload Mass | M _{pay} | Given | (kg) |
| Specific Impulse | I _{sp} | Chosen | (s) |
| Propellant Mass | M _{prop} | $M_{prop} = \frac{M_{pay} \left(e^{\left(\frac{\Delta V}{I_{sp} g_0} \right)} - 1 \right) (1 - f_{inert})}{1 - f_{inert} e^{\left(\frac{\Delta V}{I_{sp} g_0} \right)}}$ | (kg) |
| Inert Mass | M _{inert} | $M_{inert} = \frac{f_{inert}}{(1 - f_{inert})} M_{prop}$ | (kg) |
| Initial Mass | M _i | M _i = M _{pay} + M _{inert} + M _{prop} | (kg) |
| Final Mass | M _f | M _f = M _{pay} + M _{inert} | (kg) |

Table 5. Algorithm that was used in the propulsion system design, specifically in creating the Dummkopf charts.

Normally, after we have assumed an inert mass fraction, it is possible to calculate the propellant, initial, inert, and

final masses. However, the fact that this particular mission has two separate ΔV maneuvers makes it more challenging. If the mission were staged, we could apply the propulsion algorithm in Table 5 to each of the two consecutive stages. However, this mission assumes that no mass will be discarded between burns. In other words, the inert mass used in the LEO burn will be added to the payload of the GEO burn. This creates the need for iteration since the parameters of the GEO burn are dependent on those of the LEO burn, and vice versa. The algorithm used to finalize the mass breakdown of the spacecraft system is provided in Table 8. Again, this algorithm assumes that the burn at GEO will have no inert mass of its own, and all of the necessary components have already been accounted for in the LEO portion. A summary of the mass relationships for the mission example are shown in Table 6 and Table 7.

| Propellant | Isp (s) | Delta V (m/s) | Spacecraft Mass (kg) | Inert Mass (kg) | Payload (kg) | Inert Mass Fraction | Propellant Mass (kg) | Initial Mass (kg) |
|---------------------------------|------------|------------------|-------------------------|--------------------|-----------------|------------------------|-------------------------|----------------------|
| Hydrozine | 230 | 1475 | 3600 | 8468.08 | 12068.08 | 0 | 11140.28 | 23208.37 |
| H ₂ / O ₂ | 385 | 1475 | 3600 | 2115.80 | 5715.80 | 0 | 2731.99 | 8447.79 |

Table 6. Results of the mission analysis for the burn at GEO.

| Propellant | Isp (s) | Delta V (m/s) | Payload (kg) | Inert Mass Fraction | Propellant Mass (kg) | Inert Mass (kg) | Initial Mass (kg) |
|---------------------------------|------------|------------------|-----------------|------------------------|-------------------------|--------------------|----------------------|
| Hydrozine | 230 | 2448 | 23208.37 | 0.12 | 62099.31 | 8468.08 | 93775.77 |
| H ₂ / O ₂ | 385 | 2448 | 8447.79 | 0.18 | 9638.66 | 2115.80 | 20202.26 |

Table 7. Results of the mission analysis for the burn at LEO.

| Step Description | Corresponding Equation | Symbol | Description |
|--|--|---|--|
| Burn at GEO | | | |
| 1. Find the payload at GEO, assuming the inert mass is zero | $M_{pay} = M_{sc} + M_{inert}$ | M_{sc} M_{pay} M_{inert} | Satellite Mass Payload Mass LEO Inert Mass |
| 2. Find the propellant mass for the burn at GEO | $M_{prop} = M_{pay} e^{\left(\frac{\Delta V}{I_{sp} g_0}\right)}$ | ΔV I_{sp} g_0 m_{prop} | Delta-Velocity Specific Impulse Gravity Propellant mass for GEO |
| 3. Find the initial mass | $M_i = M_{pay} + M_{prop}$ | M_i | Initial Mass |
| Burn at LEO | | | |
| 4. Set payload equal to the initial weight of the GEO burn | $M_{pay2} = M_i$ | M_{pay2} | Payload of GEO burn |
| 5. Find the propellant mass | $M_{prop2} = \frac{M_{pay} \left(e^{\left(\frac{\Delta V}{I_{sp} g_0}\right)} - 1 \right) (1 - f_{inert})}{1 - f_{inert} e^{\left(\frac{\Delta V}{I_{sp} g_0}\right)}}$ | M_{prop2} | Propellant |
| 6. Find the inert mass | $M_{inert} = \frac{f_{inert}}{(1 - f_{inert})} M_{prop2}$ | f_{inert} | Inert mass fraction |
| 7. Start over in the GEO burn at step 1, adding the inert mass into the payload. | | | |
| 8. Repeat the above steps until the initial mass of the GEO burn converges with the payload mass of the LEO burn | | | |

Table 8. Algorithm used to determine the propulsion masses for the two separate burns at LEO and GEO.

Now that the propellant and inert masses have been found, the only task left in estimating the total propulsion system mass is sizing the storage tanks. In this portion of the mission analysis, I have two options for each of the technologies. For the hydrazine system, I sized the tanks using a pressurant-fed system and a pump-fed system. These methods refer to the way the propellant is fed into the propulsion system. In a pressurant-fed system, the pressurant replaces the propellant as it is used and provides a differential pressure which forces the propellants to flow into the combustion chamber. In a pump-fed system, a pump is used to move the propellant from the storage tank to the combustion chamber.

The pump-fed system is much more complicated because of the complex parts and turbomachinery; however, the system provides a huge mass savings because it eliminates the need for pressurant, the extra tank to hold the pressurant, and it also allows the propellant to be stored at a lower pressure. Since the volume is constant, added pressure doesn't increase the size of the tank, but the thickness has to be increased to account for the added stress. Overall, by reducing the storage pressure, the mass of the tank is decreased.

For this particular mission scenario, the pump-fed system would be chosen over the pressure-fed system because of the overall size of the propulsion system. The pressurant-fed scenario was added to the analysis for scaled down comparisons of smaller missions which often sacrifice the mass savings for simplicity, thus employing the pressurant-fed system.

For the gaseous H₂/O₂ system, I designed the hydrogen and oxygen tanks using two different methods. The first approach assumed that the storage tanks would be sized to hold the propellants for both of the ΔV maneuvers at the same time. The second approach sized the storage tanks based on the largest single burn (LEO). The second approach is the most practical for this mission analysis, and it demonstrates the flexibility of the URFC-based propulsion system. The URFC would have plenty of time to recharge the propellant tanks before the spacecraft was prepared for the burn at GEO. Expanding on this tank sizing strategy, a significant savings could be made by employing a URFC-based propulsion system on a mission which required a multitude of equally-sized burns.

Lastly, the H₂/O₂ system was designed as a blow-down system. This system delivers the propellants to the thrust chamber through differential pressure in the propellant tank. The key to this technology is to allow enough extra propellant to keep the tank at the operating pressure throughout the duration of the burn. This approach saves the complexity of a pressurant-fed system, but may result in a slight increase in overall mass. This extra mass is related to the fact that the excess hydrazine needed to create the differential pressure weighs more than the corresponding helium pressurant. The URFC provides a distinct advantage to the blow-down system because no pumps are needed to create the desired tank pressure. The tank pressure is provided by the electrochemically generated pressure which results when transforming a liquid (water) into a gas (H₂ and O₂).

The algorithm used to size the spherical tanks is listed in Table 9. The input parameters include the mass of the propellant, the density of the propellant, the maximum expected operating pressure of the tank, the density of the tank material, and the strength of the tank material. From these input parameters, the masses of the propellant storage tanks can be calculated. The first method calculates the mass of the tanks based on the hoop stress caused by the load applied by the pressure within the tank. This simplified approach has to be multiplied by a correction factor of 2.5 to account for complications including weld efficiencies, tank knuckles, feed-system fittings, and acceleration loading [8]. The other approach is the tank factor method which is a purely empirical formula which uses a density, volume, and weight ratio. The results of these two methods have been averaged in this mission analysis to give the most unbiased estimate of the tank masses.

The material chosen for the tank design was a carbon-graphite composite material which has a tank factor of 10,000 and a strength (F_{tu}) of 895 MPa [8]. The composite tanks were compatible with all of the propellants stored, and they offered one of the lightest design options. All of the tanks were assumed to be spherical, and each component was stored in a separate tank. The hydrazine tanks were designed with a factor of safety of four since the propellant is toxic and comes into contact with personnel during pre-launch activities. The H₂/O₂ system was designed with a factor of safety of two because the

propellants are non-toxic, resulting in less liability and damage if the tanks were to rupture.

| Parameter | Corresponding Equation | Symbols | Units |
|---|--|--------------------------|------------------------------|
| Density of propellant | constant | ρ_{prop} | (kg/m ³) |
| Mass of propellant | Previously Calculated | m_{prop} | (kg) |
| Maximum expected operating pressure of the tank | Estimated at chamber pressure + 25% system and line losses | MEOP | (Pa) |
| Design burst pressure | $P_{burst} = MEOP \times F.O.S$ (F.O.S. = Factor of Safety) | P_{burst} F.O.S. | (Pa) (none) |
| Strength of tank material | constant | Ftu | (Pa) |
| Tank volume (5% ullage, 10% margin) | $V_{tank} = 1.15 \left(\frac{m_{prop}}{\rho_{prop}} \right)$ | V_{tank} | (m ³) |
| Tank radius | $R_{tank} = \left(\frac{3V_{tank}}{4\pi} \right)^{\frac{1}{3}}$ | R_{tank} | (m) |
| Tank surface area | $S.A. = 4\pi R_{tank}^2$ | S.A. | (m ²) |
| Tank wall thickness | $T_w = \left(\frac{P_{burst} R_{tank}}{2 Ftu} \right)$ | T_w | (m) |
| Mass of tank [Hoop stress method] | $m_{hs} = S.A. T_w \rho_{mat}$ (ρ_{mat} = density of tank material) | m_{hs} ρ_{mat} | (kg) (kg/m ³) |
| Corrected hoop stress | $m_{cor} = 2.5 m_{th}$ | m_{cor} | (kg) |
| Tank Factor | chosen | ϕ_t | (none) |
| Mass of tank [tank factor] | $m_{tf} = \left(\frac{P_{burst} V_{tank}}{\phi_t g_o} \right)$ | m_{tf} g_o | (kg) (m/s ²) |
| Average mass | $m_{av} = \left(\frac{m_{cor} + m_{tf}}{2} \right)$ | m_{av} | (kg) |

Table 9. Algorithm used in sizing spherical storage tanks.

The pressurant chosen for the pressurant-fed hydrogen design was helium. Helium's characteristics allow it to be lightweight and safe. The sizing of the helium pressurant tanks was accomplished with the algorithm listed in Table 10.

| Step Description | Corresponding Equation | Symbols | Description |
|--|--|-------------------------|---|
| 1. Assume the volume of the pressurant tank is zero | N/A | V_{ptank} | Volume of pressurant tank (m^3) |
| 2. Estimate the volume of pressurant | Start with the volume of the propellant tanks + 15% | V_{press} | Volume of Pressurant (m^3) |
| 3. Select the initial temperature and pressure for the pressurant | Pick T_i , P_i , P_f greater than operating temperature and pressure | T_i P_i P_f | Initial temperature ($^\circ\text{K}$) Initial pressure (Pa) Final pressure (Pa) *for the pressurant |
| 4. Use the isotropic relationship to find T_f | $T_f = T_i \left(\frac{P_f}{P_i} \right)^{\frac{(\gamma-1)}{\gamma}}$ | T_f γ | Final pressurant temperature ($^\circ\text{K}$) Ratio of specific heats (constant of the pressurant fluid) |
| 5. Use the ideal gas law to find the mass of pressurant | $m_{press} = \frac{V_{press} P_f}{R T_f}$ | R m_{press} | Pressurant gas constant (8314 J / kgmol-K) Mass of the pressurant (kg) |
| 6. Use the ideal gas law to find V_{ptank} at initial temperature and pressure required to hold the mass of pressurant | $V_{ptank} = \frac{m_{press} R T_i}{P_i}$ | | |
| 7. Go back to step 2 until V_{ptank} converges | | | |

Table 10. Algorithm used to determine the pressurant mass and volume given the volume of the propellant tanks.

The algorithm used in sizing the pump is listed in Table 11.

It is important to remember that the storage pressure of the hydrazine was reduced from 3.45 MPa to .25 MPa for this case.

| Step Description | Corresponding Equation | Symbol | Description |
|--|--|--|--|
| 1. Determine pressure drop across injector | $P_{inj} = .20 P_c$ | P_{inj} P_c | Injector pressure drop Chamber pressure |
| 2. Estimate the turbine pressure ratio as 1.0 | $P_{trat} = 1.0$ | P_{trat} | Turbine pressure ratio |
| 3. Pump discharge pressure | $P_{td} = P_c + P_{inj}$ | P_{td} | Pump discharge pressure |
| 4. Pump inlet pressure | $P_{ip} = P_{td} * P_{trat}$ | P_{ip} | Pump inlet pressure |
| 5. Pump ΔP | $\Delta P = 1.25 (P_{ip} - P_{tank})$ | ΔP P_{tank} | Change in pressure provided by pump Chosen tank pressure |
| 6. Pump head rise | $H_p = \Delta P / (\rho g_o)$ | H_p ρ g_o | Pump head rise (m) Density of fluid Gravity |
| 7. Thrust | $F = T/W g_o m_{init}$ | F T/W m_{init} | Thrust Design thrust to weight ratio Initial vehicle mass |
| 8. Mass flow rate | $\dot{m} = \frac{F}{I_{sp} g_o}$ | I_{sp} | Propellant's specific impulse |
| 9. Power Required | $P_{req} = \frac{g_o \dot{m} H_p}{\eta_p}$ | P_{req} η_p | Required power Efficiency of the pump |
| 10. Power Output | $P_{out} = \eta_t \dot{m} C_p T_i \left[1 - \left(\frac{1}{P_{trat}} \right)^{\gamma-1} \right]$ | η_t C_p T_i γ | Turbine efficiency Specific heat (J/kg-K) Turbine inlet temp (K) Isentropic parameter |
| 11. Calculate the difference in powers | $\Delta P_f = P_{out} - P_{req}$ | ΔP_f | Difference in required and actual power |
| 12. Adjust P_{trat} in Step 2. until the power required equals the power output from the pump ($\Delta P_f < \pm 1.0E6$) | | | |

Table 11. Algorithm used to size the pump in the pump-fed

Hydrozine system.

The results of the mission example demonstrate the many advantages of the URFC-based propulsion system. The areas where the URFC technology benefited the mission included a smaller total propellant mass, a smaller amount of inert mass, and a smaller total tank mass. Adding these savings together results in a considerable savings in the total system mass. The area where the URFC technology was inferior included only the total tank volume. Because the propellants are stored in a gaseous state, there is a significant density disadvantage for the URFC-based propulsion system which results in nearly twice the required tank volume for propellant storage. Overall, the increased tank volume is acceptable in trade for the huge mass savings that the URFC system provides.

Table 12 provides a summary of the percent in mass savings over the pressurant-fed hydrazine system. The three categories represent the other three technology scenarios. The first category is the pump-fed hydrazine system. This system accounts not only for the additional weight of the pump, but also considers the weight of the additional solar arrays and batteries which would be needed to provide the pump with power during the maneuver. The second category is the H₂/O₂ system that was sized to hold the propellants for both maneuvers at the same time. Finally, the last category is the design of choice. This is a H₂/O₂ system that has been sized according to the largest ΔV maneuver, allowing the URFC to recharge the propellants between maneuvers. This design offers the optimum design, minimizing the total system mass and volume.

| <i>*Values expressed as a percent savings over the baseline pressurant-fed hydrazine system</i> | Hydrazine (Pump-fed) | H ₂ /O ₂ (Big tanks) | H ₂ /O ₂ (Small tanks) |
|---|-------------------------|---|--|
| Total propellant mass | 0.0 | 83.1 | 83.1 |
| Total inert mass | 0.0 | 75.1 | 75.1 |
| Total pressurant mass | 100.0 | 100.0 | 100.0 |
| Total tank mass | 98.9 | -35.6 | 46.1 |
| Total tank volume | 45.3 | -609.5 | -182.10 |
| Total system mass | 20.4 | 32.7 | 67.2 |

Table 12. The mission example results. A comparison of the different propulsion systems, expressed as a percent savings over the baseline hydrogen pressurant-fed system.

A more complete table of values can be referenced in the assortment of spreadsheets and graphs included in Appendix A. Included in the spreadsheets are values for each of the systems, outlining the mass distributions of each subcategory. There are also spreadsheets which outline the propellant, tank, and pump sizing algorithms. A graph of the Dummkopf chart which was used to analyze the feasibility of the mission is included, as well as the spreadsheet which was used to create it. Finally, a series of graphs were created to show the savings by category of the specific technologies. These graphs allow a better visualization of the advantages and disadvantages of the URFC-based propulsion system.

As a final note in this mission analysis, the URFC could be employed as the battery source without any noticeable change in mass. In a mission of this magnitude, the 10% propellant margin which was accounted for in mission planning would be more than enough to provide adequate electrical power to the spacecraft for the duration of the mission. Although not calculated, the elimination of batteries would save a notable amount of spacecraft mass. Overall, this one of the many advantages of the URFC-based integrated propulsion system.

4.0 Discussion of Limitations

The biggest limitation in the development of the URFC integrated propulsion and power system is that it lacks flight heritage. In order to be selected as a technology aboard a spacecraft, a system must be flight proven; however, that same system must be selected in order to gain flight experience. This loop must be broken through research, and this is currently limited by a lack of funding. However, the use of fuel cells on the ground as power plants, and the ever-increasing interest in zero-emission vehicles is greatly advancing the URFC technology. This limitation may be solved in the near future.

Aside from the political/bureaucratic limitations, the most important physical limitation on the URFC system is the volume of the tanks. As we saw in the mission example, gaseous oxygen and hydrogen cannot be stored very efficiently. This offered the only category where the URFC system did not drastically improve the mission. I assumed that the gaseous hydrogen and oxygen were

stored near 0°C, so lowering this temperature could reduce the density of the gasses and result in a smaller tank volume. Also, the possibility of cryogenic storage is feasible if the system is large enough. A study by Lisa Kohout showed a system savings of over 50% in storing the H₂ and O₂ propellants cryogenically in a lunar base mission [10]. She concluded that the added equipment needed to liquefy the H₂ and O₂ would not be feasible on a simple earth-orbiting mission.

Lastly, the water which provides the fuel to the URFC must be maintained above the freezing temperature. Depending on the mission, this may require an intricate system of radiators and heaters. In comparison, most batteries have strict operating temperatures, so this is not a URFC-specific problem.

5.0 Discussion of Applications

There are many applications for the URFC integrated propulsion and power system. As this paper has demonstrated, URFCs offer a tremendous mass savings in both the propulsion system and the battery system. These mass savings are not limited by the duration or altitude of the mission. In fact, the URFC system actually favors complex missions with a variety of different ΔV maneuvers. A variety of small maneuvers allows the URFC system to employ smaller storage tanks which can be refilled on demand.

The flexibility of the propulsion and power system allow a spacecraft to better adapt to the type of anomalies that would doom a traditional system. An example of the flexibility is the

trade between the stored energy capacity and ΔV capability. Overall, the efficiency of the URFC system provides it an opportunity to be used in a variety of completely different applications, even small satellites.

5.1 IMPRESS System for Small Satellites

URFC technology has even been applied to the field of small satellites. A team of scientists from Lawrence Livermore National Laboratory created a system that meets the demands of small satellites quite efficiently. The integrated modular propulsion and regenerative electro-energy storage system (IMPRESS) is a unique integrated system designed for small satellites. This system uses a H₂/O₂ URFC as a storage mechanism for both electrical energy and gH₂/gO₂ propellants. Figure 13 shows the IMPRESS system schematic.

In addition to the efficiencies discussed previously in this paper, the IMPRESS system also saves mass by integrating a third major spacecraft component, the structural component. The IMPRESS system uses a piped framework as the storage tanks for the gaseous H₂ and O₂. This is a very practical approach since the small satellites require very little propellant for orbit maintenance and attitude control. Of course, the piped system may add weight to the structural component; however, the combined system is much more efficient than having a separate storage tank. In most cases, the design also allows more flexibility in the physical dimensions of the spacecraft. It is much easier to intertwine the pipes in the structure than position a spherical

or cylindrical tank. This aspect may prove important on missions where the spacecraft depends on riding piggyback during launch, or is trying to fit into one of the Space Shuttle's payload compartments.

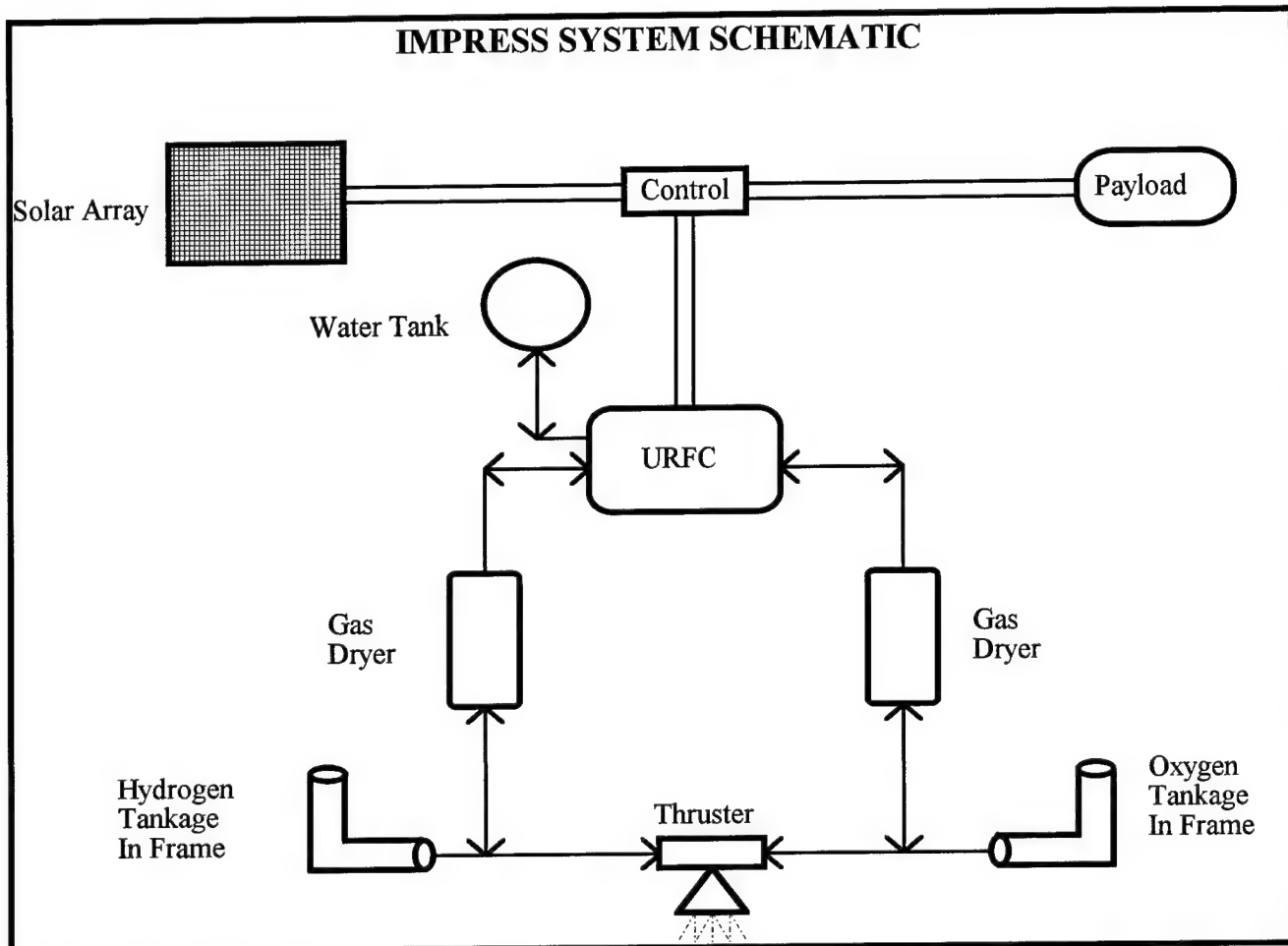


Figure 13. The IMPRESS multifunctional system combines three major spacecraft functional elements: propulsion, power, and structure [2].

6.0 Conclusion

URFC technology will revolutionize future spacecraft and mission design. The efficiency demonstrated by the URFC is unparalleled in any separate propulsion and power system today. The significant design gains of the URFC system include:

- Reduced spacecraft mass
- Improved mission flexibility
- Very high I_{sp} propellants
- Improved mission safety and reduced factors of safety
- Non-toxic propellants
- Double the specific energy storage capacity of state of the art batteries; over four times the storage of current technology
- System does not suffer the same mission life limitations that batteries do
- Generation of O_2 for manned mission scenarios
- Generation of H_2 for attitude control and orbit maintenance

Overall, the URFC system provides advantages which cannot be ignored. The system has not only proven itself on paper, but it is currently gaining recognition in ground-based applications and demonstrations. The next step for this technology is an experimental space mission. I strongly urge this next step, as it will provide a breakthrough in propulsion and power system performance.

Appendix A

| | |
|---|-----|
| Propulsion System Mass Spreadsheet..... | A-1 |
| Dummkopf Spreadsheet and Charts..... | A-2 |
| Hohmann Transfer Summary..... | A-3 |
| Tank Sizing Spreadsheet..... | A-4 |
| Pump Sizing Spreadsheet..... | A-5 |
| Summary and Comparison of Technologies..... | A-6 |

Appendix (A-1): Spreadsheet used to determine the propulsion masses.
Reference Table 8, pg 34, to see the corresponding algorithm used.

| Burn at GEO | | | | | |
|---------------------------------|------------|------------------|-------------------------|--------------------|-----------------|
| Propellant | Isp (s) | Delta V (m/s) | Spacecraft Mass (kg) | Inert Mass (kg) | Payload (kg) |
| Hydrozine | 230 | 1475 | 3600 | 8468.08843 | 12068.088 |
| H ₂ / O ₂ | 385 | 1475 | 3600 | 2115.8046 | 5715.8046 |

Gravity (m/s²) 9.80665

| Burn at LEO | | | | | |
|---------------------------------|------------|------------------|-----------------|------------------------|-------------------------|
| Propellant | Isp (s) | Delta V (m/s) | Payload (kg) | Inert Mass Fraction | Propellant Mass (kg) |
| Hydrozine | 230 | 2448 | 23208.372 | 0.12 | 62099.315 |
| H ₂ / O ₂ | 385 | 2448 | 8447.7959 | 0.18 | 9638.6654 |

Difference:
 Hydrozine:
 H₂ / O₂: 0.000321
 3.95E-05

1

2

3

4

5

6

7

8

9

10

11

12

13

14

15

16

17

18

19

20

21

22

23

24

25

26

27

28

29

30

31

32

33

34

35

36

37

38

39

40

41

42

43

44

45

46

47

48

49

50

51

52

53

54

55

56

57

58

59

60

61

62

63

64

65

66

67

68

69

70

71

72

73

74

75

76

77

78

79

80

81

82

83

84

85

86

87

88

89

90

91

92

93

94

95

96

97

98

99

100

101

102

103

104

105

106

107

108

109

110

111

112

113

114

115

116

117

118

119

120

121

122

123

124

125

126

127

128

129

130

131

132

133

134

135

136

137

138

139

140

141

142

143

144

145

146

147

148

149

150

151

152

153

154

155

156

157

158

159

160

161

162

163

164

165

166

167

168

169

170

171

172

173

174

175

176

177

178

179

180

181

182

183

184

185

186

187

188

189

190

191

192

193

194

195

196

197

198

199

200

201

202

203

204

205

206

207

208

209

210

211

212

213

214

215

216

217

218

219

220

221

222

223

224

225

226

227

228

229

230

231

232

233

234

235

236

237

238

239

240

241

242

243

244

245

246

247

248

249

250

251

252

253

254

255

256

257

258

259

260

261

262

Appendix (A-2): Spreadsheet used to calculate the values needed to create the Dummkopf chart. Following that, there are two separate Dummkopf charts, one for hydrazine and one for H₂/O₂.

F(inert) = .10

| Gravity Force (m/sec ²) | Delta V Required (m/s) | Initial Inert Mass Fraction (no units) | Payload Mass (kg) | ISP Values (s) | Propellant Mass (kg) | Inert Mass (kg) | Initial Mass (kg) |
|--|---------------------------|---|----------------------|-------------------|-------------------------|--------------------|----------------------|
| 9.80665 | 2448 | 0.1 | 8447.7959 | 100 | 1000000 | 1000000 | 1000000 |
| | | 0.12 | | 125 | 183853.87 | 20428.208 | 212729.8712 |
| | | 0.14 | | 150 | 68983.289 | 7664.8099 | 85095.89459 |
| | | 0.16 | | 175 | 41216.668 | 4579.6297 | 54244.09338 |
| | | 0.18 | | 200 | 28981.156 | 3220.1284 | 40649.08039 |
| | | 0.2 | | 230 | 21173.352 | 2352.5947 | 31973.74304 |
| | | 0.22 | | 255 | 17215.162 | 1912.7958 | 27575.75423 |
| | | | | 280 | 14468.073 | 1607.5637 | 24523.43284 |
| | | | | 305 | 12456.778 | 1384.0864 | 22288.66026 |
| | | | | 330 | 10924.236 | 1213.8041 | 20585.83645 |
| | | | | 355 | 9719.7867 | 1079.9763 | 19247.55895 |
| | | | | 385 | 8577.7505 | 953.08339 | 17978.62984 |
| | | | | 410 | 7809.2427 | 867.69363 | 17124.73224 |
| | | | | 435 | 7164.8999 | 796.09999 | 16408.79578 |
| | | | | 460 | 6617.1924 | 735.2436 | 15800.2319 |
| | | | | 485 | 6146.1119 | 682.90132 | 15276.80907 |
| | | | | 510 | 5736.7794 | 637.41993 | 14821.99522 |

F(inert) = .12

| ISP Values | Propellant Mass | Inert Mass | Initial Mass |
|------------|-----------------|------------|--------------|
| 100.0 | 1000000.0 | 1000000.0 | 1000000.0 |
| 125.0 | 408186.9 | 55681.9 | 472296.6 |
| 150.0 | 86903.5 | 11850.5 | 107201.7 |
| 175.0 | 47008.4 | 6410.2 | 61866.5 |
| 200.0 | 31730.0 | 4326.8 | 44504.6 |
| 230.0 | 22604.0 | 3082.4 | 34134.2 |
| 255.0 | 18149.1 | 2474.9 | 29071.8 |
| 280.0 | 15122.1 | 2062.1 | 25632.0 |
| 305.0 | 12938.6 | 1764.3 | 23150.7 |
| 330.0 | 11293.0 | 1540.0 | 21280.8 |
| 355.0 | 10010.6 | 1365.1 | 19823.5 |
| 385.0 | 8803.5 | 1200.5 | 18451.8 |
| 410.0 | 7995.9 | 1090.3 | 17534.0 |
| 435.0 | 7321.7 | 998.4 | 16767.9 |
| 460.0 | 6750.7 | 920.6 | 16119.1 |
| 485.0 | 6261.1 | 853.8 | 15562.7 |
| 510.0 | 5836.9 | 795.9 | 15080.6 |

F(inert) = .14

| ISP Values | Propellant Mass | Inert Mass | Initial Mass |
|------------|-----------------|------------|--------------|
| 100.0 | 1000000.0 | 1000000.0 | 1000000.0 |
| 125.0 | 1000000.0 | 1000000.0 | 1000000.0 |
| 150.0 | 119349.7 | 19429.0 | 147226.5 |
| 175.0 | 55113.1 | 8971.9 | 72532.8 |
| 200.0 | 35226.6 | 5734.6 | 49408.9 |
| 230.0 | 24324.0 | 3959.7 | 36731.5 |
| 255.0 | 19241.6 | 3132.3 | 30821.7 |
| 280.0 | 15873.0 | 2584.0 | 26904.7 |
| 305.0 | 13484.3 | 2195.1 | 24127.3 |
| 330.0 | 11706.6 | 1905.7 | 22060.1 |
| 355.0 | 10334.3 | 1682.3 | 20464.4 |
| 385.0 | 9052.8 | 1473.7 | 18974.3 |
| 410.0 | 8201.0 | 1335.1 | 17983.9 |
| 435.0 | 7493.3 | 1219.8 | 17161.0 |
| 460.0 | 6896.4 | 1122.7 | 16466.8 |
| 485.0 | 6386.2 | 1039.6 | 15873.6 |
| 510.0 | 5945.4 | 967.9 | 15361.1 |

F(inert) = .16

| ISP Values | Propellant Mass | Inert Mass | Initial Mass |
|------------|-----------------|------------|--------------|
| 100.0 | 1000000.0 | 1000000.0 | 1000000.0 |
| 125.0 | 1000000.0 | 1000000.0 | 1000000.0 |
| 150.0 | 196020.9 | 31910.4 | 236379.1 |
| 175.0 | 67261.9 | 10949.6 | 86659.3 |
| 200.0 | 39824.1 | 6483.0 | 54754.9 |
| 230.0 | 26431.0 | 4302.7 | 39181.5 |
| 255.0 | 20536.6 | 3343.2 | 32327.6 |
| 280.0 | 16744.0 | 2725.8 | 27917.5 |
| 305.0 | 14107.8 | 2296.6 | 24852.2 |
| 330.0 | 12173.6 | 1981.8 | 22603.2 |
| 355.0 | 10696.5 | 1741.3 | 20885.6 |
| 385.0 | 9329.6 | 1518.8 | 19296.1 |
| 410.0 | 8427.5 | 1371.9 | 18247.3 |
| 435.0 | 7682.0 | 1250.6 | 17380.3 |
| 460.0 | 7055.8 | 1148.6 | 16652.3 |
| 485.0 | 6522.7 | 1061.8 | 16032.4 |
| 510.0 | 6063.6 | 987.1 | 15498.5 |

F(inert) = .18

| ISP Values | Propellant Mass | Inert Mass | Initial Mass |
|------------|-----------------|------------|--------------|
| 100.0 | 1000000.0 | 1000000.0 | 1000000.0 |
| 125.0 | 1000000.0 | 1000000.0 | 1000000.0 |
| 150.0 | 600821.9 | 131887.7 | 741157.4 |
| 175.0 | 87487.9 | 19204.7 | 115140.4 |
| 200.0 | 46139.7 | 10128.2 | 64715.7 |
| 230.0 | 29072.1 | 6381.7 | 43901.5 |
| 255.0 | 22096.3 | 4850.4 | 35394.5 |
| 280.0 | 17766.5 | 3900.0 | 30114.2 |
| 305.0 | 14826.7 | 3254.7 | 26529.2 |
| 330.0 | 12705.2 | 2789.0 | 23942.0 |
| 355.0 | 11104.8 | 2437.6 | 21990.3 |
| 385.0 | 9638.7 | 2115.8 | 20202.3 |
| 410.0 | 8678.9 | 1905.1 | 19031.9 |
| 435.0 | 7890.3 | 1732.0 | 18070.1 |
| 460.0 | 7231.2 | 1587.3 | 17266.3 |
| 485.0 | 6672.3 | 1464.7 | 16584.8 |
| 510.0 | 6192.6 | 1359.4 | 15999.8 |

F(inert) = .20

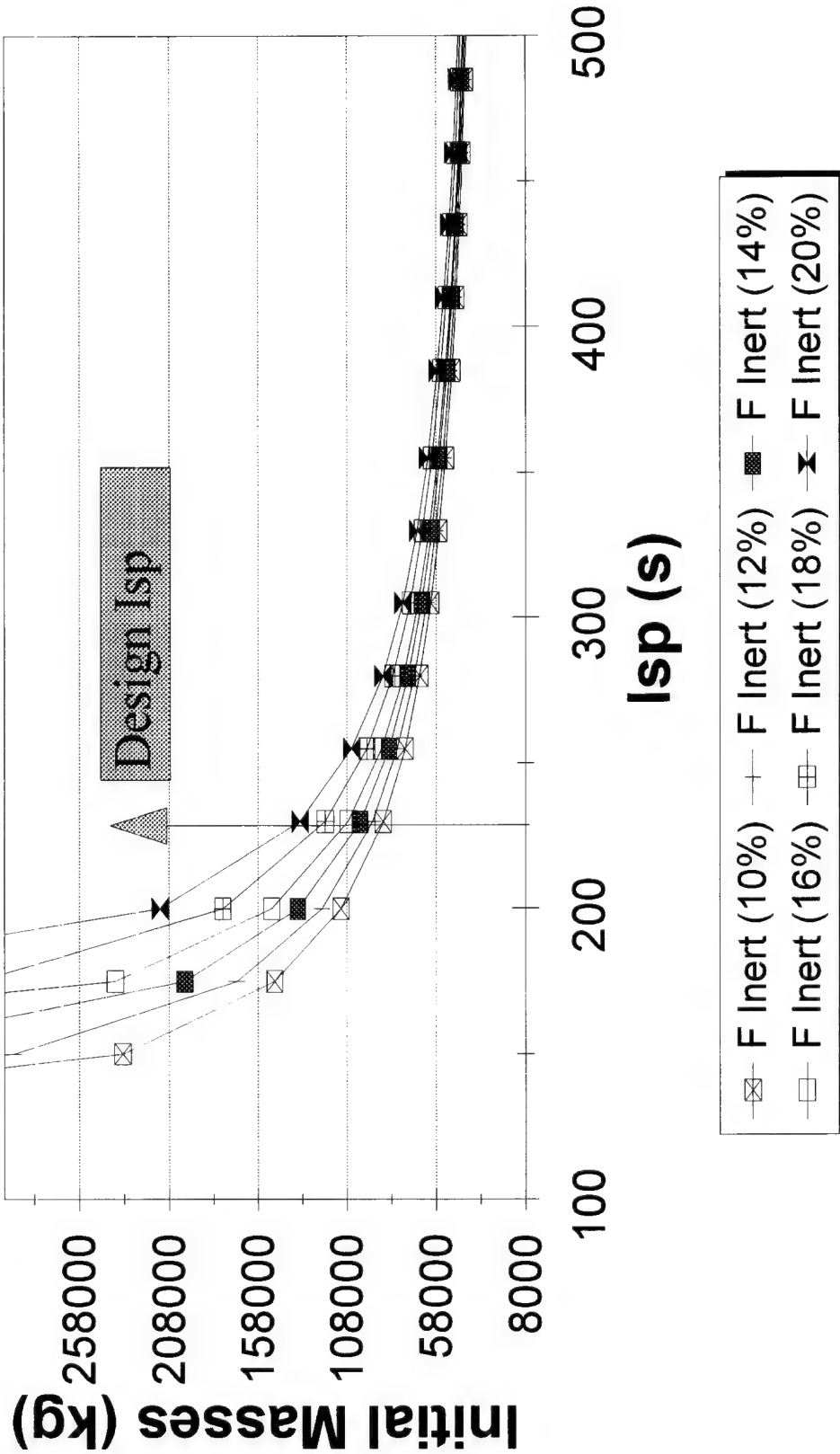
| ISP Values | Propellant Mass | Inert Mass | Initial Mass |
|------------|-----------------|------------|--------------|
| 100.0 | 1000000.0 | 1000000.0 | 1000000.0 |
| 125.0 | 1000000.0 | 1000000.0 | 1000000.0 |
| 150.0 | 1000000.0 | 1000000.0 | 1000000.0 |
| 175.0 | 127857.8 | 31964.5 | 168270.1 |
| 200.0 | 55357.7 | 13839.4 | 77644.9 |
| 230.0 | 32479.8 | 8120.0 | 49047.6 |
| 255.0 | 24011.1 | 6002.8 | 38461.6 |
| 280.0 | 18983.7 | 4745.9 | 32177.4 |
| 305.0 | 15665.0 | 3916.2 | 28029.0 |
| 330.0 | 13315.8 | 3329.0 | 25092.6 |
| 355.0 | 11568.4 | 2892.1 | 22908.3 |
| 385.0 | 9986.0 | 2496.5 | 20930.3 |
| 410.0 | 8959.6 | 2239.9 | 19647.3 |
| 435.0 | 8121.6 | 2030.4 | 18599.8 |
| 460.0 | 7425.0 | 1856.2 | 17729.0 |
| 485.0 | 6837.0 | 1709.2 | 16994.0 |
| 510.0 | 6334.2 | 1583.6 | 16365.6 |

F(inert) = .22

| ISP Values | Propellant Mass | Inert Mass | Initial Mass |
|------------|-----------------|------------|--------------|
| 100.0 | 1000000.0 | 1000000.0 | 1000000.0 |
| 125.0 | 1000000.0 | 1000000.0 | 1000000.0 |
| 150.0 | 1000000.0 | 1000000.0 | 1000000.0 |
| 175.0 | 248314.9 | 70037.5 | 326800.2 |
| 200.0 | 70075.6 | 19764.9 | 98288.4 |
| 230.0 | 37044.9 | 10448.6 | 55941.2 |
| 255.0 | 26417.7 | 7451.1 | 42316.6 |
| 280.0 | 20457.1 | 5769.9 | 34674.8 |
| 305.0 | 16654.8 | 4697.5 | 29800.1 |
| 330.0 | 14024.3 | 3955.6 | 26427.7 |
| 355.0 | 12099.5 | 3412.7 | 23960.0 |
| 385.0 | 10379.3 | 2927.5 | 21754.6 |
| 410.0 | 9274.8 | 2616.0 | 20338.6 |
| 435.0 | 8379.8 | 2363.5 | 19191.1 |
| 460.0 | 7640.2 | 2154.9 | 18242.9 |
| 485.0 | 7019.0 | 1979.7 | 17446.6 |
| 510.0 | 6490.2 | 1830.6 | 16768.5 |

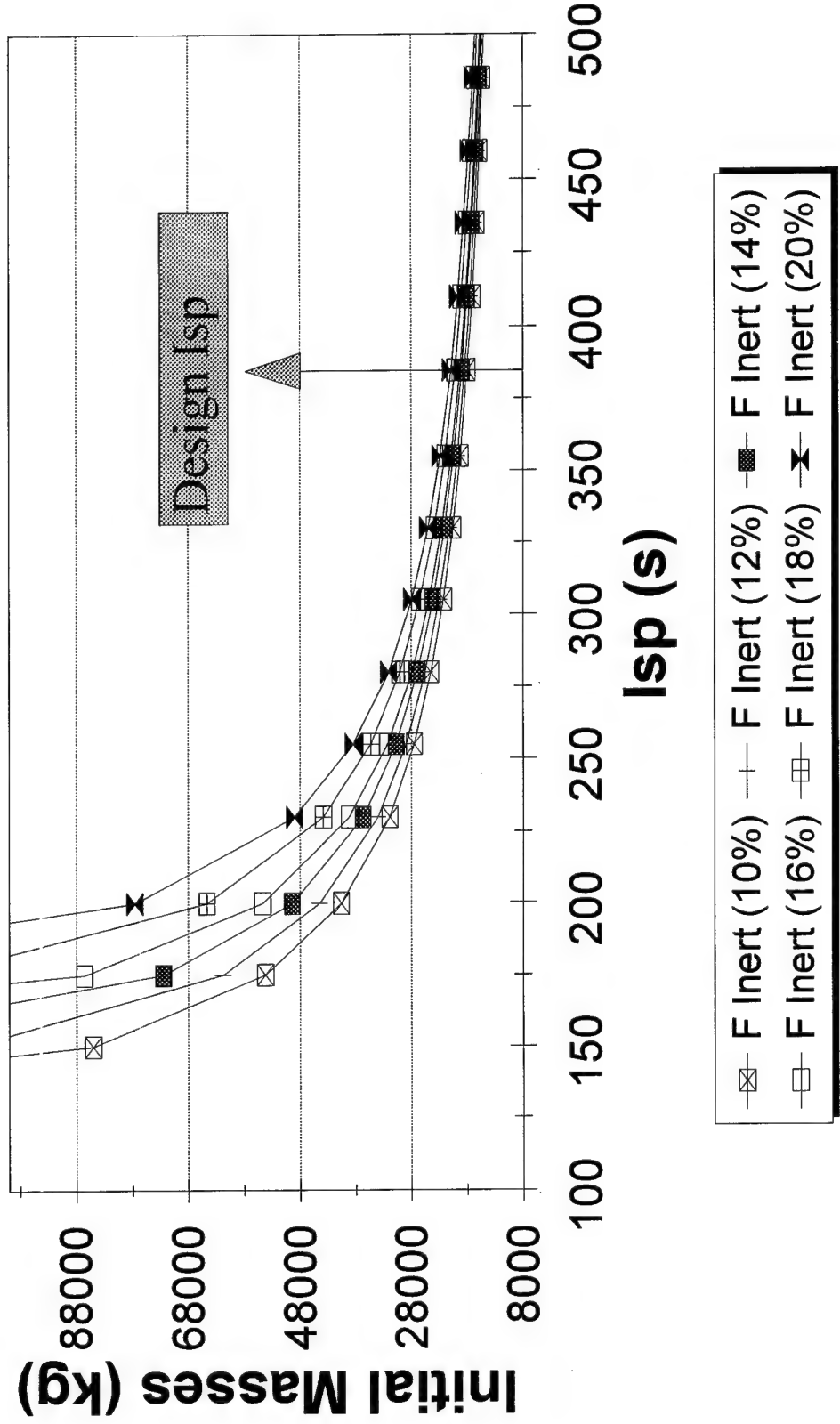
Dummkopf Chart

Burn at LEO for Hydrazine



Dummkopf Chart

Burn at LEO for H₂ / O₂



Appendix (A-3): The Hohmann transfer spreadsheet.
Reference Table 4, pg 30, for the corresponding algorithm used.

| Hohmann Transfer Summary | | | | | | |
|--------------------------|---|---------|----------------------|-----------------|-----------|----------------------|
| | Fuel Type | Isp | Spacecraft Mass (kg) | Inert Mass (kg) | Payload | Propellant Mass (kg) |
| Burn at GEO | Hydrozine H ₂ / O ₂ | 230,000 | 3600,000 | 8468,088 | 12068,088 | 1140,284 |
| | | 385,000 | 3600,000 | 2115,805 | 5715,805 | 2731,991 |
| Burn at LEO | Hydrozine H ₂ / O ₂ | 230,000 | **** | 8468,088 | 23208,372 | 23208,372 |
| | | 385,000 | **** | 2115,805 | 8447,796 | 8447,796 |

Appendix (A-4) Tank sizing spreadsheets and results.

Reference Table 9, pg 38, for the corresponding algorithm that was used.

Pressurant Mass and Volume

| | |
|----------------------------------|----------------------|
| Vol. Propellant Tanks (m^3) | 83.391622642 |
| Vol. Pressurant Tank (m^3) | 60.548942115 |
| Vol. Pressurant w/ 5% Margin | 151.13759299 |
| Initial Temperature (K) | 300 |
| Initial Pressurant Pressure (Pa) | 2.10E+07 (From Book) |
| Final Pressurant Pressure (Pa) | 4600000 |
| Gamma Helium | 1.66 |
| Final Temperature (K) | 164.03092473 |
| Mass of Pressurant (kg) | 2039.6660003 |
| R for Helium (kJ/kg°K) | 2078 |
| Vol. Pressurant Tank (m^3) | 60.548942123 |
| Difference in Volumes (m^3) | 8.463942E-09 |

50%

Ideal Gas Law

| Storage Temp (K) | Hydrogen (H ₂)g | Oxygen (O ₂)g | (8:1 O/F ratio by mass used) (60 F) |
|------------------|-----------------------------|---------------------------|--|
| 273 | 273 | 273 | Match Temps |
| 8314 | 8314 | 8314 | |
| 4600000 | 4600000 | 4600000 | |
| 2 | 32 | | |
| 1374.5174152022 | 10996.13932162 | | |
| 339.10569746387 | 169.5528487319 | | |
| 4.053359838782 | 64.85375742051 | | |

1298 - 20 °C

Tank Sizing (Helium Pressure Fed System)

| | Hydrazine (Pressure Fed) | Pressurant | Hydrazine (Pump Driven) | Water (40 F) | Hydrogen (g) Big Tank | Oxygen (g) Big Tank | Hydrogen (g) Small Tank | Oxygen (g) Small Tank | Graphite Density |
|-------------------------------------|-----------------------------|------------|----------------------------|--------------------|--------------------------|------------------------|----------------------------|--------------------------|------------------|
| Density (kg/m^3) | 1010 | 33.9123 | 1010 | 1000.0326684363 | 4.053359838782 | 64.85375742051 | 4.05335983888 | 64.8537574205 | 1550 |
| Mass (kg) | 73239.599016 | 2039.666 | 73239.59902 | 12370.65673682 | 1374.5174152022 | 10996.13932162 | 1070.9628218 | 8567.7025747 | |
| MEOP tank (Pa) [Chamber + 25%] | 4600000 | 2100000 | 250000 | 4600000 | 4600000 | 4600000 | 4600000 | 4600000 | |
| Design Burst Pressure (Pa) | 18400000 | 8400000 | 1000000 | 9200000 | 9200000 | 9200000 | 9200000 | 9200000 | |
| Ftu (Pa) | 895000000 | 895000000 | 895000000 | 895000000 | 895000000 | 895000000 | 895000000 | 895000000 | |
| Volume (m^3) | 83.391622642 | 69.1671134 | 83.39162264 | 14.225790513011 | 712.12196467414 | 356.0609823371 | 277.42687737 | 138.713438685 | |
| (5% Ullage / 10% Propellant Margin) | | | | | | | | | |
| Radius (m) | 2.7102619734 | 2.54646091 | 2.710261973 | 1.5031278906742 | 5.5397299036312 | 4.396886538322 | 4.0459450003 | 3.21126867487 | |
| Surface Area (m^2) | 92.306526227 | 81.4861675 | 92.30652623 | 28.392375528268 | 385.64441429213 | 242.9407576705 | 205.70735194 | 129.587511413 | |
| Wall Thickness (m) | 0.0278596762 | 0.11949872 | 0.001514113 | 0.0077255735163142 | 0.028472354811959 | 0.02259852299 | 0.0207948011 | 0.01650484459 | |
| Mass of Tank [Hoop Stress] (kg) | 3986.0263873 | 15093.1142 | 216.6318689 | 339.98844589197 | 17019.317122212 | 8509.658561106 | 6630.3473821 | 3315.17369103 | |
| Corrected Hoop Stress (x 2.5) (kg) | 9965.0659682 | 37732.7856 | 541.5796722 | 849.97111472993 | 42548.29280553 | 21274.14640277 | 16575.868455 | 8287.93422757 | |
| Tank Factor (Max.) | 10000 | 10000 | 10000 | 10000 | 10000 | 10000 | 10000 | 10000 | |
| Mass of Tank [tank factor] (kg) | 15646.585293 | 59245.8946 | 850.3578963 | 1334.5767690262 | 66806.932795624 | 33403.46639781 | 26026.494999 | 13013.2474994 | |
| Average of Tank and Hoop (kg) | 12805.825631 | 48489.3401 | 695.9687843 | 1092.2739418781 | 54677.612800577 | 27338.80640029 | 21301.181727 | 10650.5908635 | |

Pressure of Helium in
Ullage

Appendix (A-5): Pump sizing spreadsheets.

Reference Table 11, pg 40, for the corresponding algorithm used.

Pump Sizing

| | | |
|-------------------------------|--------------|---|
| "Hydrazine" | | |
| Chamber Pressure (Pa) | 3450000 | |
| Injector Pressure Drop (Pa) | 690000 | (20% of Chamber Pressure) |
| Turbine Pressure Ratio | 1.0748131656 | |
| Pump Discharge Pressure (Pa) | 4140000 | |
| Pump Inlet Pressure (Pa) | 4449726.5055 | |
| Pump Delta-Pressure (Pa) | 5249658.1319 | (25% system losses) |
| Pump Head Rise (m) | 530.01599106 | |
| Tank Pressure (Pa) | 250000 | (Chosen from suggested range [0.2-0.5 MPa]) |
| Density of Hydrazine (kg/m^3) | 1010 | |

Power Balance

| | | |
|------------------------------|--------------|----------------------------------|
| Pump Efficiency | 0.8 | (Standard Value - Hydrogen) |
| Turbine Efficiency | 0.7 | (Standard Value) |
| Thrust to Weight Ratio (T/W) | 0.3 | |
| Thrust (N) | 275887.86278 | |
| Mass Flow Rate (kg/s) | 122.31622897 | |
| Pump Power Required (W) | 794701.0 | |
| Turbine Pressure Ratio | 1.0748131656 | |
| Molecular Weight (kg/kg-mol) | 32 | (Assume Propellant Temp = 300 K) |
| Cp (J/kg-K) | 962.0050 | |
| Gamma | 1.37 | 1.370001816 |
| Turbine Inlet Temp (K) | 500 | (225-650 K on page 213 SPAD) |
| Power Out from Turbine | 794701.0 | |
| Difference in Powers | 4.657777E-07 | |

Turbopump Sizing

| | | |
|--------------------------------|--------------|-----------------------------------|
| Pump Head Rise (m) | 530.01599106 | |
| Pump Power Required (W) | 794700.97289 | |
| Volumetric Flow Rate (m^3 / s) | 0.1211051772 | |
| Pump Speed (rad/s) | 634.84158983 | (one stage pump) |
| Pump Torque (N-m) | 1251.8098777 | |
| Pump Mass (kg) | 108.29646571 | (A=1.5 and B=0.6 on pg. 266 SPAD) |

Appendix (A-6): A summary of the example mission. Comparisons are made by category on the basis of weight saved and by percent saved over the baseline pressurant-fed hydrazine system. Following the spreadsheet is a series of graphs which illustrate the savings gained by using the URFC system.

Overall System Comparison

| | Total Delta-V (m/s) | Total Propellant Mass (kg) | Total Inert Mass (kg) | Total Pressurant Mass (kg) | Total Tank Volume (m ³) | Total System Mass (kg) | Solar Arrays (kg) | Pump (kg) | Batteries (kg) |
|---|------------------------|-------------------------------|--------------------------|-------------------------------|--|---------------------------|----------------------|--------------|-------------------|
| Hydrazine (Press) | 3923.00 | 7329.60 | 8468.09 | 2039.67 | 61285.17 | 152.56 | 145042.52 | ***** | ***** |
| Hydrazine (Pump) | 3923.00 | 7329.60 | 8468.09 | **** | 695.97 | 83.39 | 115419.95 | 31788.00 | 108.30 |
| H ₂ / O ₂ (Big) | 3923.00 | 12310.66 | 2115.80 | **** | 83108.69 | 1082.41 | 97595.15 | **** | **** |
| H ₂ / O ₂ (Small) | 3923.00 | 12310.66 | 2115.80 | **** | 33044.05 | 430.37 | 47530.51 | **** | **** |

*The 3 above additional categories were added to the pump-fed system because of the increased power needed by the pump.

Savings by Category

| | | | | | | |
|------------------|----------|---------|---------|-----------|---------|----------|
| Hydrazine (Pump) | 0.00 | 0.00 | 2039.67 | 60599.20 | 69.17 | 29622.57 |
| Big Tanks | 60868.94 | 6352.28 | 2039.67 | -21873.53 | -929.85 | 47447.36 |
| Small Tanks | 60868.94 | 6352.28 | 2039.67 | 28251.12 | -277.81 | 97512.01 |

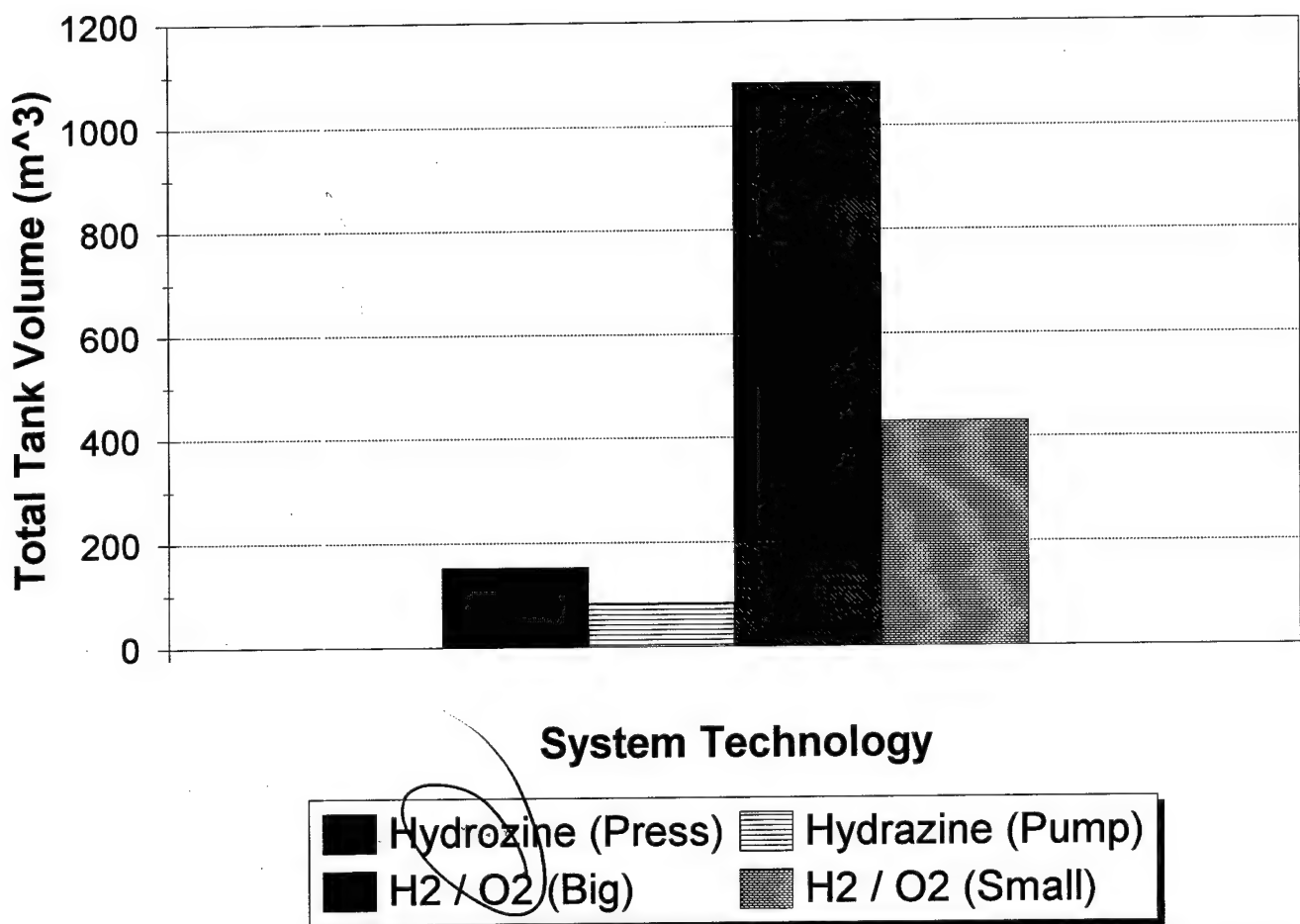
*Boxed areas highlight where URFC technology is inferior

Percent Reduced

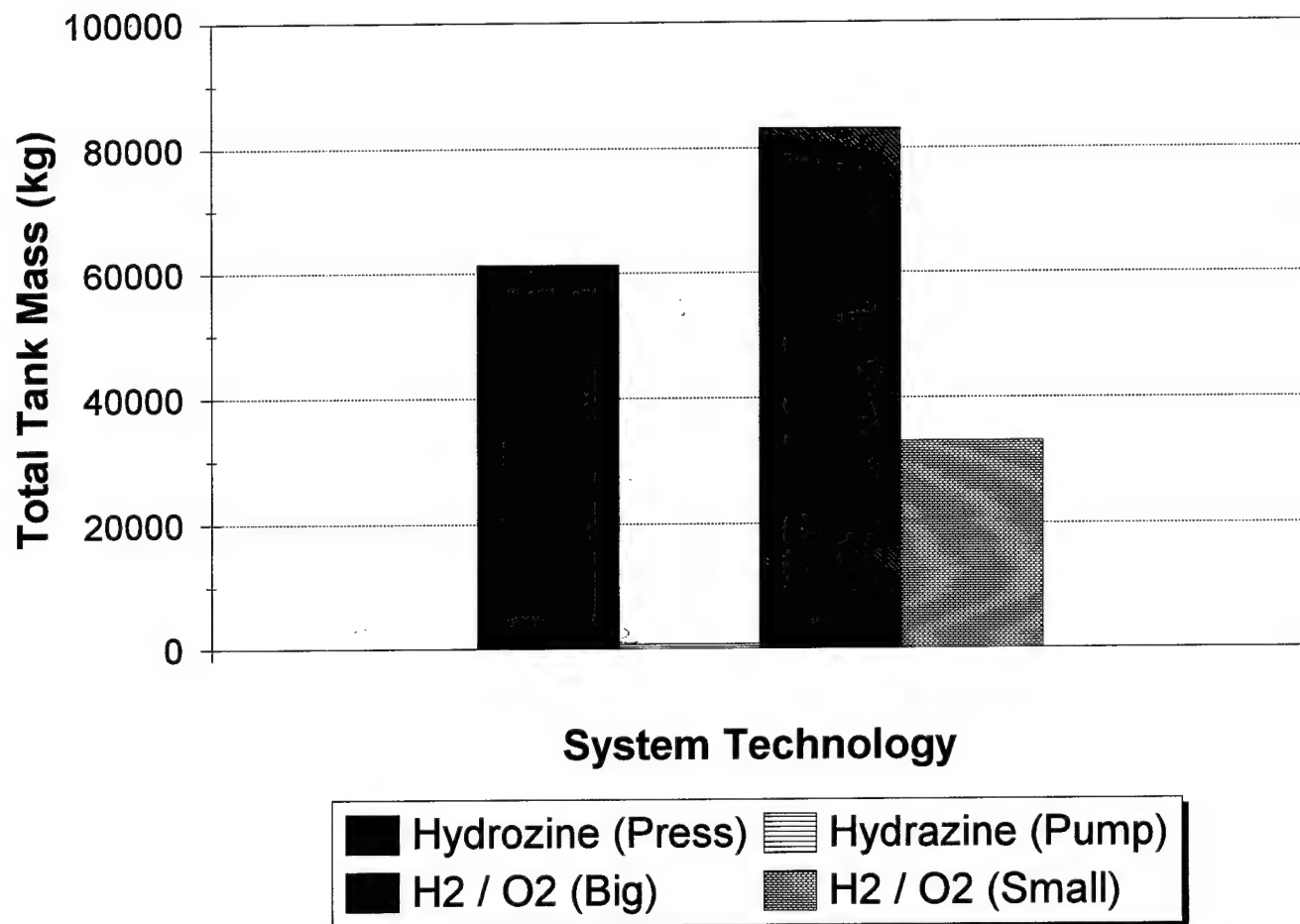
| | | | | | | |
|------------------|-------|-------|--------|--------|---------|-------|
| Hydrazine (Pump) | 0.00 | 0.00 | 100.00 | 98.86 | 45.34 | 20.42 |
| Big Tanks | 83.11 | 75.01 | 100.00 | -35.59 | -609.50 | 32.71 |
| Small Tanks | 83.11 | 75.01 | 100.00 | 46.09 | -182.10 | 67.23 |

*Boxed areas highlight where URFC technology is inferior

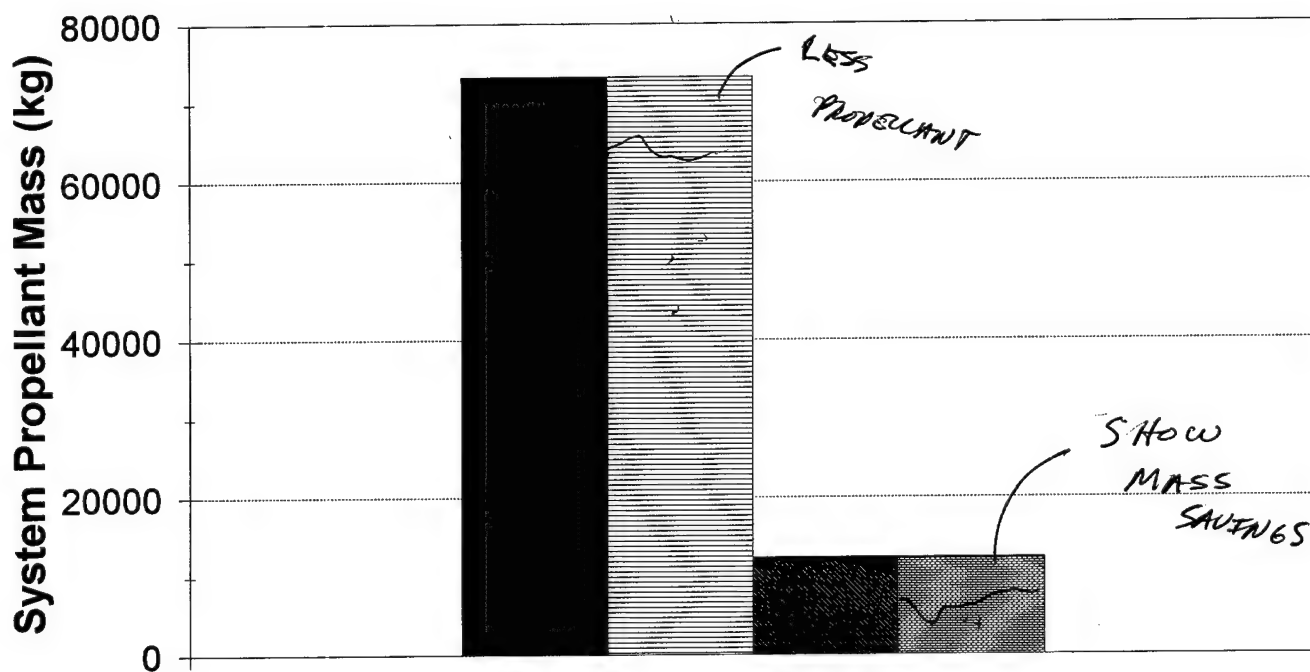
Propulsion Storage Tank Comparison



Propulsion Storage Tank Comparison



System Propellant Mass Comparison

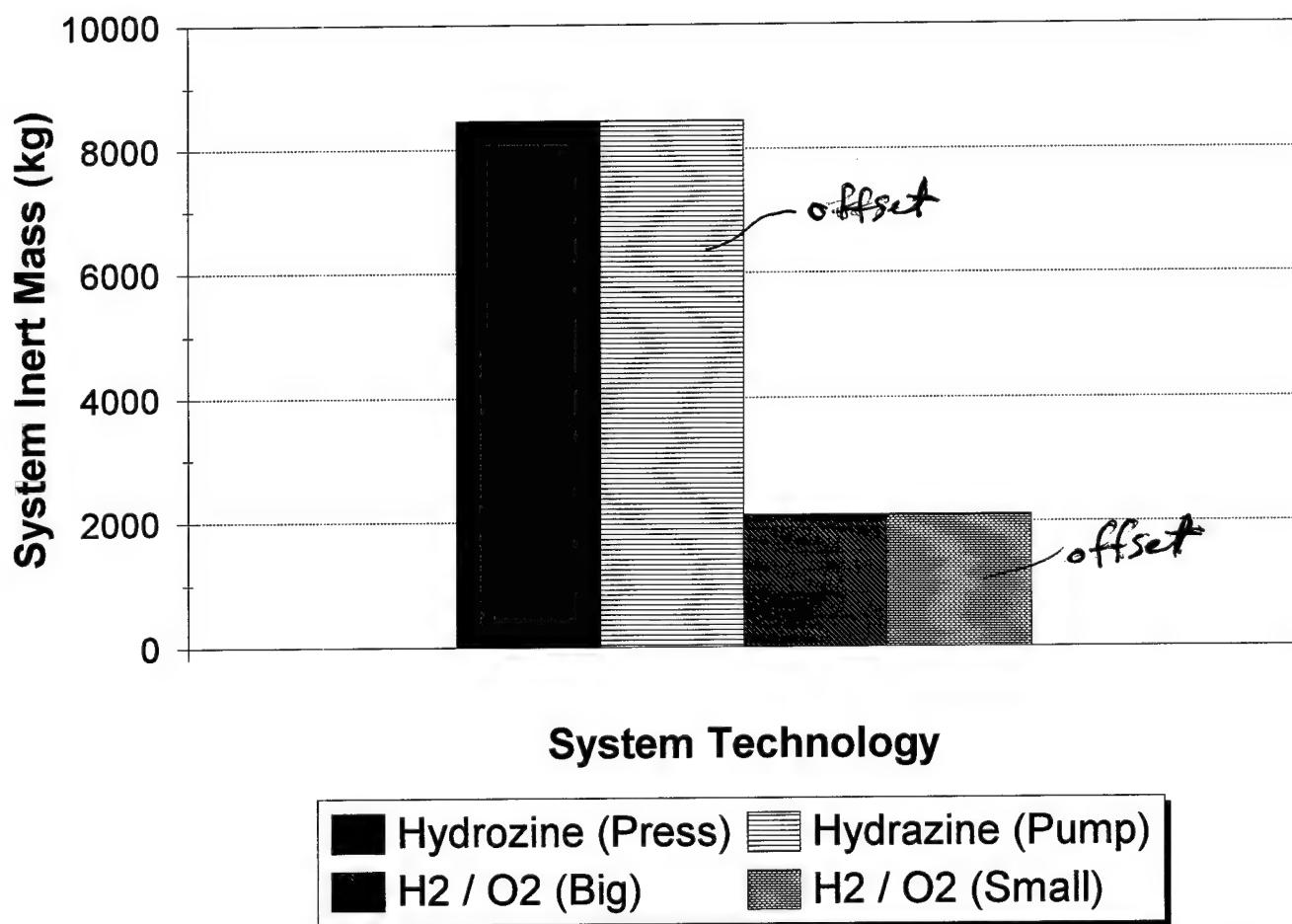


System Technology

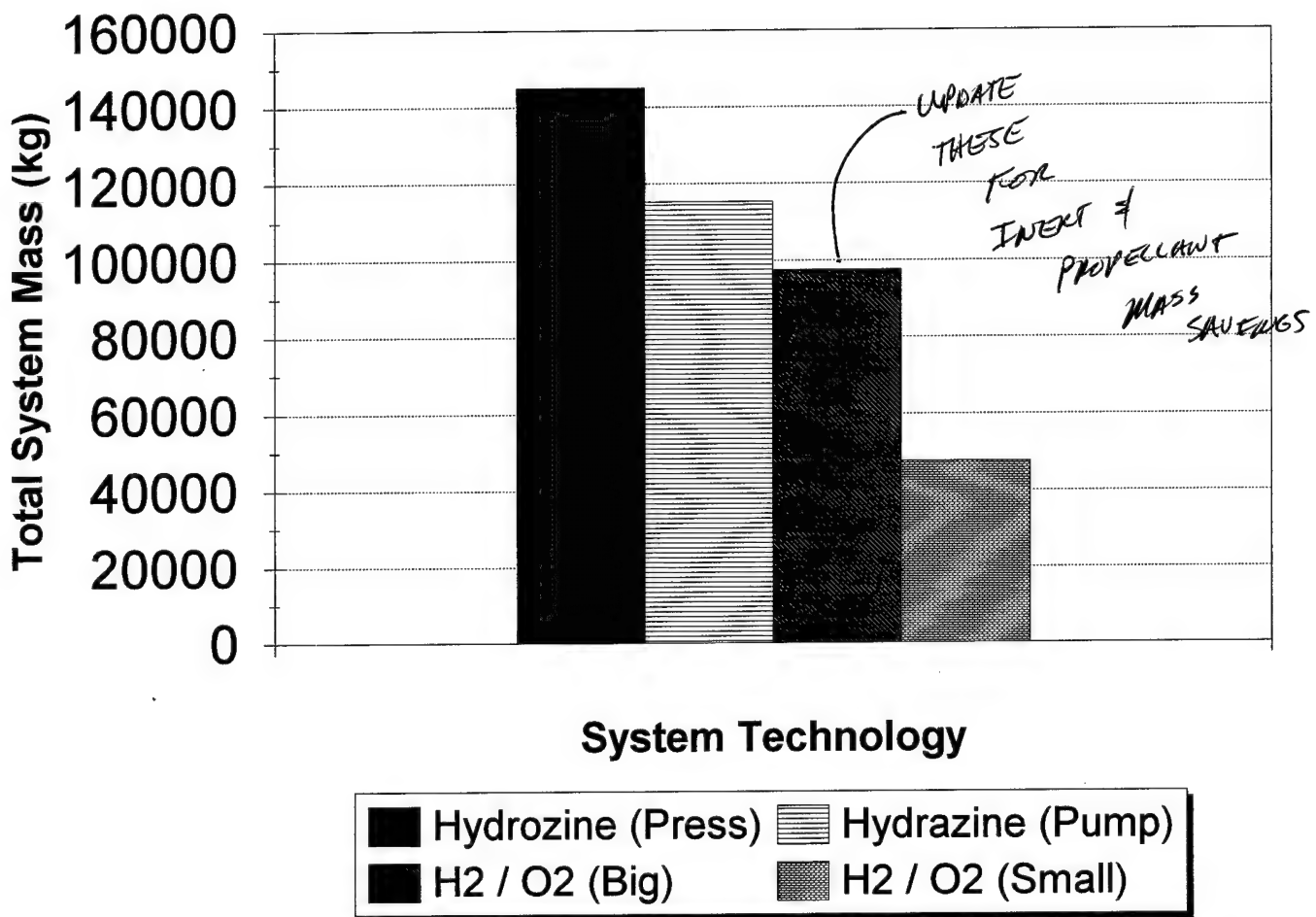
| | |
|---------------------------------------|---|
| Hydrozine (Press) | Hydrazine (Pump) |
| H ₂ / O ₂ (Big) | H ₂ / O ₂ (Small) |

O₂, H₂

System Inert Mass Comparison



Total System Mass Comparison



Bibliography

- [1] Fuel Cell. "Fuel Cell Descriptions".
<http://www.dodfuelcell.com/fcdescriptions.html>
- [2] Mitlitsky, Fred, Wim de Groot, LeRoy Butler, and James McElroy. "Integrated Modular Propulsion and Regenerative Electro-Energy Storage System (IMPRESS) for Small Satellites". LLNL, Livermore, California, 1997.
- [3] Walter, Katie. "The Unitized Regenerative Fuel Cell".
<http://www.llnl.gov/str/Mitlit.html>
- [4] Nasier, Clay. Power-Lamar 3/1/96 Progress Report.
"Power-Lamar 3/1/96 Progress Report"
<http://www.ae.utexas.edu/~tsgc/power/p0301.html>
- [5] The Fuel Cell Future. "Fuel Cell Info". International Fuel Cells.
<http://www.hamilton-standard.com/ifc-onsi/cell/pem.html>
- [6] Mitlitsky, F., and B. Myers, and A.H. Weisberg, "Lightweight Pressure Vessels and Unitized Regenerative Fuel Cells", LLNL, Livermore, California, UCRL-JC-125220 (November 1996). Presented at the 1996 Fuel Cell Seminar, San Diego, California, November 17-20, 1996.
- [7] Larson, Wiley, and James Wertz. Space Mission Analysis and Design. 2nd ed., Microcosm, Inc., California and Kluwer Academic Publishers, Boston, 1992. pp. 391-409
- [8] Humble, Ronald, Gary Henry, and Wiley Larson. Space Propulsion Analysis and Design, McGraw-Hill, Inc., New York, 1995.
- [9] Vallado, David. Fundamentals of Astrodynamics and Applications. McGraw-Hill, Inc., New York, 1995. pp. 281
- [10] Kohout, Lisa. "Cryogenic Reactant Storage for Lunar Base Regenerative Fuel Cells". Cryogenic Storage Paper, Lewis Research Center, Cleveland, Ohio, NASA TM 101980 (June 1989). Prepared for the International Conference on Space Power sponsored by the International Astronautical Federation, Cleveland, Ohio, June 5-7, 1989.
- [11] Fuel Cells 2000. "Types of Fuel Cells".
<http://www.fuelcells.org/fctypes.shtml>

- [12] Artemis Data Book. "Electrical Power Systems / Regenerative Fuel Cell Data".
<http://www.asi.org/adb/04/03/03/rfc-data.html>
Artemis Society International, 1996.
- [13] Olliver, Viktor. Artmis Data Book. "Electrical Powere Systems / Hydrogen-Oxygen Fuel Cells for Lunar habitat Energy Storage".
<http://www.asi.org/adb/04/03/03/h2power.html>
Artemis Society International, 1997.
- [14] Mars Power System Paper. "Fuel Cell / Electrolyzer Subsystem".
<http://powerweb.lerc.nasa.gov/psi/DOC/mspaper.html>

Unitized Regenerative Fuel Cells (URFCs)

2Lt. J.R. Coalson
29 April 1998

Master of Engineering Space Operations
University of Colorado at Colorado Springs

Purpose of Investigation

Demonstrate how URFC technology can meet the increasing demands to reduce spacecraft mass, increase mission flexibility, and increase reliability.

Overview

- Background
- Description of URFC Technology
- How URFCs Compare to Batteries
- The Gaseous H₂/O₂ Propulsion System
- Safety of the URFC System
- Mission Example
- Conclusions

Background

- Uses the water cycle to form electricity and rocket propellants
- Combines both the propulsion and energy (battery) subsystems
- Operates dually as a fuel cell and an electrolyzer

Background

- Energy Storage (Fuel Cell)
 - Energy is stored in the H₂ and O₂ fuel
 - Fuel passed through a catalyst to form H₂O
 - Electrochemically generated DC energy
- Propellant Storage (Electrolyzer)
 - Stored as H₂O
 - H₂O is electrolyzed to produce H₂ and O₂
 - Gaseous H₂ and O₂ are burned as propellant

Background

- Fuel cells have been used since the 1960s
 - Gemini
 - Apollo
 - Space Shuttle
- The regenerative option was overlooked
 - Currently, URFCs are not space qualified
 - Limited funding for research

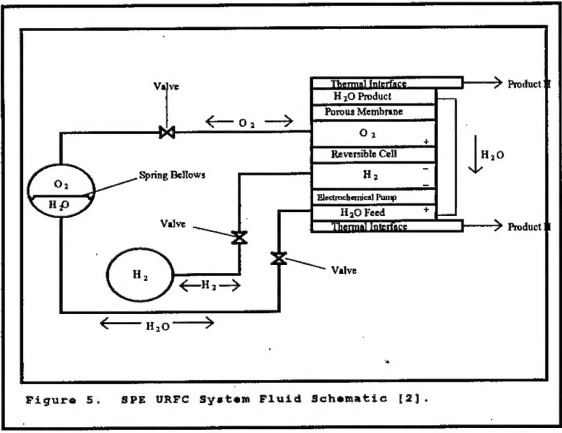


Figure 5. SPE URFC System Fluid Schematic [2].

URFCs vs. Batteries

- Advantages

- Higher specific energy storage
- URFCs are unaffected by DOD or cycle length
- Increased flexibility

- Disadvantages

- Not flight proven
- Proton Exchange Membrane durability

| Battery/URFC System | Theoretical Specific Energy (Wh/kg) | Packaged Specific Energy (Wh/kg) | Comments |
|---------------------|-------------------------------------|----------------------------------|--|
| H_2/O_2 URFC | 3660 | 400-1000 | URFCs with light-weight pressure vessels |
| Li-SPE/ MnO_2 | 735 | 220 | Novel packaging for unmanned systems |
| Ag/Zn | 450 | 200 | Excess Zn required, low charge rate |
| Lithium | 700 | 100 | Larger cells offer marginal improvement |
| Ni/MH_x | 470 | 70 | MH_x is metal hydride. Low specific energy |
| Ni/H_2 | 470 | 60 | Low specific energy |
| Ni/Cd | 240 | 60 | Low specific energy |

Table 2. Theoretical and Packaged Specific Energy for URFCs and State-of-the-Art Rechargeable Batteries [2].

$$Cr = \frac{P_e T_e}{(DOD) N n} (W-hr)$$

Parameter Descriptions

- Cr = Required battery capacity in W-hrs per battery
- P_e = Average eclipse load (W)
- T_e = Maximum eclipse time (hr)
- DOD = Limit on battery's depth-of-discharge
- N = Number of batteries (non-redundant)
- n = Transmission efficiency between battery and load

Figure 7. Estimate of the Required Capacity of Secondary Batteries [8].

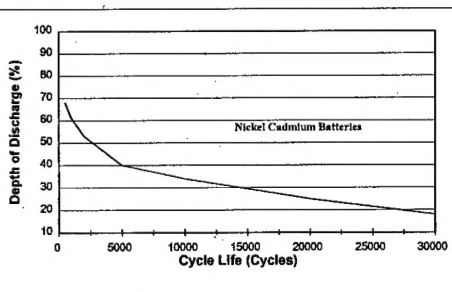


Figure 8. Depth-of-discharge versus cycle life for Nickel Cadmium Batteries [7].

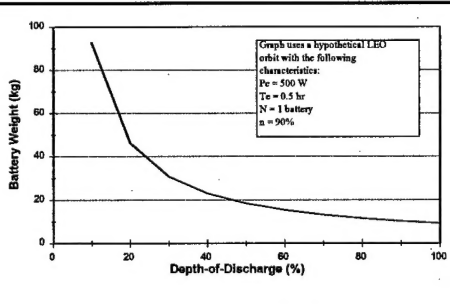


Figure 9. Battery mass versus the allowable depth-of-discharge.

Gaseous H₂/O₂ Propulsion System

- Advantages

- Propellants with high I_{sp} values
- Flexible and controllable ΔV maneuvers
- Nontoxic propellants
- No turbo-pumps required
- Increased system flexibility

Gaseous H₂/O₂ Propulsion System

- Disadvantages

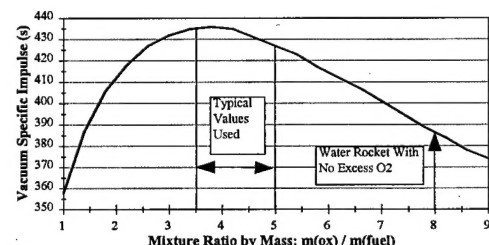
- Not flight proven
- Tank size

| Chemical Technology | Specific Impulse (I _{sp}) in Seconds |
|--|--|
| Liquid Fluorine/Hydrogen | 390-440 |
| Gaseous or Liquid Hydrogen/Oxygen | 360-435 |
| Gaseous Hydrogen/Oxygen Burnt at an O/F of 8:1 | 385 |
| All Other Liquid Bipropellants | 320-360 |
| All Hybrid Technologies | 290-350 |
| All Solid Technologies | 260-300 |
| All Liquid Monopropellants | 140-235 |

Table 3. A comparison of I_{sp} values for chemical propellants [8].

Vacuum Isp vs. Mixture Ratio

"Fuel = H₂ (g) Oxidizer = O₂ (g)"



Safety of URFC System

- Non-toxic propellants

- Reduced liability during testing
- Allows integrated system testing
- Allows the reduction of factors of safety
- No environmental or political roadblocks

Mission Example

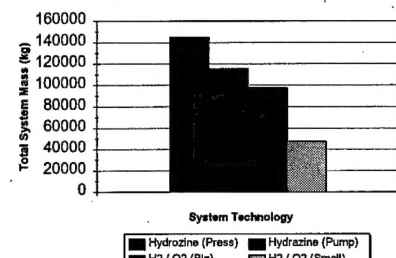
- Hypothetical Mission

- Transfer a 3,600 kg satellite from LEO to GEO
- Use a simple Hohmann transfer
- Compare URFC technology to that of Hydrazine
- Focus on propellant and storage tank masses
- Assumed that the mass of the other components was negligible

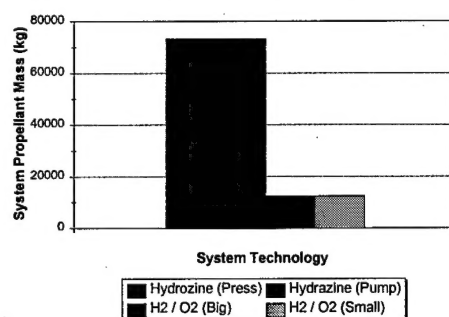
Mission Example

- Four different configurations were considered
 - Pressure-fed hydrazine system
 - Pump-fed hydrazine system
 - Large H₂/O₂ system
 - Small H₂/O₂ system

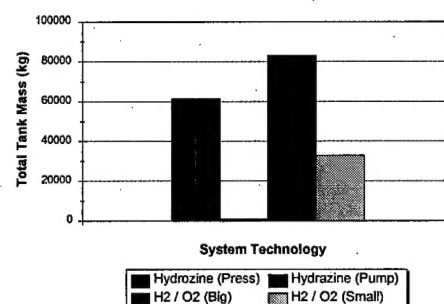
Total System Mass Comparison



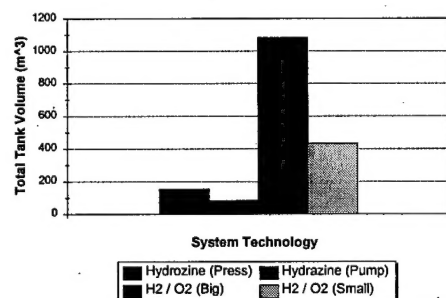
System Propellant Mass Comparison



Propulsion Storage Tank Comparison



Propulsion Storage Tank Comparison



Conclusions

- URFC Technology offers many advantages
 - Reduced spacecraft mass
 - Improved mission flexibility
 - Improved mission safety and reliability
- The only major system downfall is in the area of flight heritage

Recommendation

- We need to apply URFC technology to an experimental space mission
- The sooner we develop flight experience, the sooner we can benefit from this technology